in this curve at $T\cong 0.37$ °K and a maximum at $T\cong 0.08$ °K. The predicted minimum has recently been found (at $T=0.32$ °K) in the experiment of Baum, Brewer, Daunt, and Edwards.[24] *Note added in proof.*—See in addition S. G. Sydoriak, R. L. Mills, and E. R. Grilly, Phys. Rev. Letters 4, 495 (1960), and D. M. Lee, H. A. Fairbank, and E. J. Walker, Bull. Am. Phys. Soc. 4, 239 (1959), whose experiments show this minimum at 0.330 °K and 0.32 °K, respectively. We also consider the influence of an external magnetic field on the melting curve and find that very high fields ($\approx 10^6$ gauss) are required for an appreciable effect.

PHYSICAL REVIEW VOLUME 119, NUMBER 3 AUGUST 1, 1960

Lattice Dynamics of Alkali Halide Crystals*

A. D. B. Woods, W. Cochran,† and B. N. Brockhouse
Physics Division, Atomic Energy of Canada Limited, Chalk River, Ontario, Canada
(Received March 11, 1960)

The paper comprises theoretical and experimental studies of the lattice dynamics of alkali halides. A theory of the lattice dynamics of ionic crystals is given based on replacement of a polarizable ion by a model in which a rigid shell of electrons (taken to have zero mass) can move with respect to the massive ionic core. The dipolar approximation then makes the model exactly equivalent to a Born-von Kármán crystal in which there are two "atoms" of differing charge at each lattice point, one of the "atoms" having zero mass. The model has been specialized to the case of an alkali halide in which only one atom is polarizable, and computations of dispersion curves have been carried out for sodium iodide. We have determined the dispersion $\nu(\mathbf{q})$ relation of the lattice vibrations in the symmetric [001], [110], and [111] directions of sodium iodide at 110°K by the methods of neutron spectrometry. The transverse acoustic, longitudinal acoustic, and transverse optic branches were determined completely with a probable error of about 3%. The dispersion relation for the longitudinal optic (LO) branch was determined for the [001] directions with less accuracy. Frequencies of some important phonons with their errors (units 10^{12} cps) are: TA[0,0,1]1.22 ± 0.04, LA[0,0,1] 1.82 ± 0.06, TA[$\frac{1}{2},\frac{1}{2},\frac{1}{2}$]$1.52\pm0.05$, LA[$\frac{1}{2},\frac{1}{2},\frac{1}{2}$]$2.32\pm0.06$, TO[0,0,0] $3.6_0\pm0.1$, TO[0,0,1]$3.8_0\pm0.1$, TO[$\frac{1}{2},\frac{1}{2},\frac{1}{2}$]$3.5_0\pm0.1$. The agreement between the experimental results and the calculations based on the shell model, while not complete, is quite satisfactory. The neutron groups corresponding to phonons of the LO branch were anomalously energy broadened, especially for phonons of long wavelength, suggesting a remarkably short lifetime for the phonons of this branch.

1. INTRODUCTION

THE lattice dynamics of a crystal is described by a frequency, wave vector dispersion relation, insofar as it is harmonic. In the last few years it has become possible to determine experimentally this dispersion relation using x-ray diffraction and neutron spectrometry. The dispersion relation has been measured fairly accurately for several metallic[1–4] and semiconducting[5–7] crystals consisting of one kind of atom. The only determinations for crystals having more than one kind of atom[8,9] have been by x-ray diffraction methods. However, there is good reason to believe that neutron measurements are much more accurate than are x-ray measurements for crystals with more than one atom per unit cell. Thus it seems desirable to study such crystals by neutron spectrometry.

In the determination of the dispersion relation by neutron spectrometry energy distributions of initially monoenergetic neutrons are measured after scattering by a single crystal in known orientation. The frequencies ν and wave vectors $\mathbf{q}$ of the vibrations are inferred from conservation of energy and momentum between the neutrons and single phonons.[3,10,11] If the frequencies and wave vectors of the phonons are well defined, then sharp groups (broadened of course by imperfect resolution) are observed in the neutron energy distributions. The center of a neutron group is taken to define the energy (E') and wave vector ($\mathbf{k}'$) of those neutrons which had interacted with a particular vibration. The frequency and wave vector of the vibration are given by the conservation equations

$$\begin{aligned} E_0-E' &= \pm h\nu \equiv \pm\hbar\omega, \\ \mathbf{Q}\equiv\mathbf{k}_0-\mathbf{k}' &= 2\pi\boldsymbol{\tau}-\mathbf{q}, \end{aligned} \tag{1.1.1}$$

where E_0 and $\mathbf{k}_0$ are the energy and momentum of the incident neutrons, and $\boldsymbol{\tau}$ is any vector of the reciprocal

* This paper was presented at the Washington, D. C., Meeting of the American Physical Society, April 30–May 2, 1959 [Bull. Am. Phys. Soc. 4, 246 (1959)].

† Visiting scientist from the Cavendish Laboratory, Cambridge, England, now returned.

[1] E. H. Jacobsen, Phys. Rev. **97**, 654 (1955). Earlier references to x-ray work are given here.

[2] C. B. Walker, Phys. Rev. **103**, 547 (1956).

[3] B. N. Brockhouse and A. T. Stewart, Revs. Modern Phys. **30**, 236 (1958). Earlier references to neutron work are given here.

[4] B. N. Brockhouse, T. Arase, G. Caglioti, M. Sakamoto, R. N. Sinclair, and A. D. B. Woods, Bull. Am. Phys. Soc. **5**, 39 (1960).

[5] B. N. Brockhouse and P. K. Iyengar, Phys. Rev. **111**, 747 (1958).

[6] A. Ghose, H. Palevsky, D. J. Hughes, I. Pelah, and C. M. Eisenhauer, Phys. Rev. **113**, 49 (1959).

[7] B. N. Brockhouse, Phys. Rev. Letters **2**, 256 (1959).

[8] H. Cole, J. Appl. Phys. **24**, 482 (1953).

[9] D. Cribier, Ann. phys. **4**, 333 (1959).

[10] R. Weinstock, Phys. Rev. **65**, 1 (1944).

[11] G. Placzek and L. Van Hove, Phys. Rev. **93**, 1207 (1954).

lattice. (For the cubic crystals we shall consider, $\tau=(1/a)(h,k,l)$ where h, k, l are a set of Miller indices and a is the cubic lattice constant.)

In addition to determining the $\nu(\mathbf{q})$ relation, it is important to assign observed phonons to the proper branch of the dispersion relation (e.g., longitudinal or transverse, acoustical or optical). This can be done to some extent from measured intensities of the observed neutron groups and consideration of crystal symmetry, but in general the intensities, and therefore the assignments to branches, are sensitive to the details of the interionic forces. Thus, it is very helpful to the conduct of the experiments to have dispersion curves and intensities computed from some reasonably realistic model of the crystal.[5] A calculated dispersion relation also makes easier the initial steps in the determination of the experimental relation by the method of successive approximation.[5]

The simplest and best understood of the crystals containing two or more different kinds of atoms are unquestionably the alkali halides with the sodium chloride structure. According to the Born theory of ionic crystals,[12] the atoms are ions with unit (positive or negative) charge, the binding being largely due to the Coulomb interaction between the ions, and the crystal being stabilized by short-range repulsive forces between nearest neighbors. The positive and negative ions lie on two interpenetrating face-centered cubic lattices, which together make up a simple cubic lattice if the difference between the ions is ignored. The crystal has the full symmetry of the face-centered cubic lattice, facilitating both experiment and calculations.

The lattice dynamics of the NaCl structure has been discussed by Lyddane and Herzfeld,[13] Iona,[14] Kellermann,[15] Born and Huang,[16] and very recently by Lundquist, Lundström, Tenerz, and Waller.[17] Kellermann computed the complete lattice dynamics for a system of point ions interacting with Coulomb forces and with central repulsive forces between nearest (unlike) neighbors. Lyddane and Herzfeld in addition took into account the fact that the ions themselves are polarized by the electric fields accompanying the lattice vibrations. However, they neglected the fact that the overlap forces between ions depend on the state of polarization of the ions, and conversely. Thus they obtained incorrect results. This point has been discussed for the special case of long waves ($q \rightarrow 0$) by Born and Huang.

In this paper we present (Sec. 2) a theory of the lattice dynamics of ionic crystals which takes account of the polarizability of the ions for vibrations of all wavelengths. The theory is based on a model of an ionic crystal already used by Dick and Overhauser[18] and by Hanlon and Lawson[19] in studies of the dielectric properties of alkali halides, and by one of us[20] in a study of the lattice vibrations of germanium. Calculations from the model in its simplest form—Coulomb forces between all ions, each having unit (positive or negative) charge, and a short-range central repulsive force between nearest neighbors only—give dispersion curves in good but not complete agreement with the experimental results on sodium iodide. In this simple form the number of parameters is sufficiently small (three) that they are entirely fixed by the accurately measured elastic constant c_{11} and the high- and low-frequency dielectric constants. By consideration of more complicated force models we are to some extent able to fix limits on the ionic character of sodium iodide, and on the degree to which noncentral first neighbor forces, and second neighbor forces, are important.

Sodium iodide was chosen for study for the following reasons:

1. The ratio of the masses of the two constituent atoms is large. Hence the optical and acoustical branches are well separated in frequency, a fact convenient for the experiments and desirable for study of the properties of the two types of vibrations.
2. The polarizability of the sodium ions is negligibly small compared with that of the iodine ions, resulting in simplification of theoretical calculations.
3. Large single crystals are commercially available.
4. The neutron scattering properties are acceptable, which is not the case for all alkali halides.

Both iodine and sodium have reasonably small capture, the scattering by iodine is almost coherent, and the scattering by sodium is about 50% coherent. Thus, about 70% of the scattering by NaI is coherent. However, the 50% incoherent scattering by the sodium atoms produces a troublesome background scattering at energy transfers corresponding to the optical modes. (Since in the optical modes the light element moves farther, it causes most of the scattering. See Sec. 3.) This is especially serious since it turns out that the transverse optical mode has an almost constant frequency, and therefore this component of the incoherent scattering appears as a neutron group in the energy distributions at all scattering angles and crystal orientations. This contaminant neutron group must be subtracted quantitatively from all other groups representing phonons in this energy range.

[12] For a comprehensive elementary treatment see F. Seitz, *The Modern Theory of Solids* (McGraw-Hill Book Company, New York, 1940), Chap. II.
[13] R. H. Lyddane and K. F. Herzfeld, Phys. Rev. **54**, 846 (1938).
[14] M. Iona, Jr., Phys. Rev. **60**, 822 (1941).
[15] E. W. Kellermann, Phil. Trans. Roy. Soc. (London) **238**, 513 (1940).
[16] M. Born and K. Huang, *Dynamical Theory of Crystal Lattices* (Oxford University Press, New York, 1954).
[17] S. O. Lundqvist, V. Lundström, E. Tenerz, and I. Waller, Arkiv Fysik **15**, 193 (1959). See also J. R. Hardy, Phil. Mag. **4**, 1278 (1959).
[18] B. J. Dick and A. W. Overhauser, Phys. Rev. **112**, 90 (1958).
[19] J. E. Hanlon and A. W. Lawson, Phys. Rev. **113**, 472 (1959).
[20] W. Cochran, Phys. Rev. Letters **2**, 495 (1959); Proc. Roy. Soc. (London) **A253**, 260 (1959).

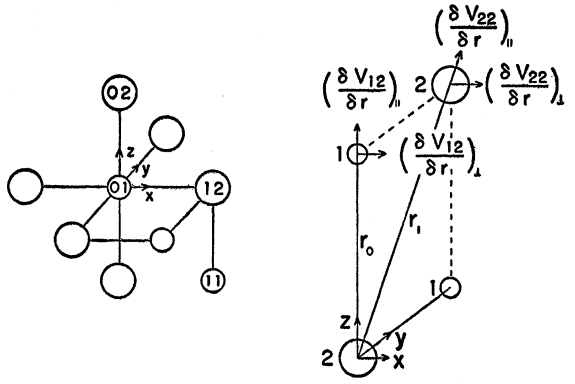

(a) (b)

FIG. 1. (a) Values of l and of κ for near-neighbor atoms. (b) Illustrates the notation used to define the gradients of short-range potentials. The atoms shown are all in the yz plane.

Measurements are presented (Sec. 4) of the dispersion relation of sodium iodide at a temperature of 110°K in the three directions of highest symmetry [001], [111], and [110]. The acoustical and transverse optical branches behaved in the way exprected from theory. For the longitudinal optical branch we obtained the unexpected result that even at the low temperature of 110°K the neutron groups were not sharp, but energy broadened. This result suggests (Sec. 5) that at temperatures down to 110°K, at least, the longitudinal optical phonons have rather short lifetimes. This effect is to be investigated in a separate publication.

2. LATTICE VIBRATION THEORY

In this section we present theoretical calculations of the dispersion curves for two models; the point ion model often considered before, and the so-called shell model[18–20] in which the polarizability of the ions is specifically taken into account. This model is specialized to the case in which only one ion—for NaI the iodine ion—is polarizable. Theoretical discussions of several topics which are not directly applicable to the experimental work on sodium iodide are given in three appendixes. These topics include a discussion of the effects of ionic polarizability on elastic constants, the effects of introducing noncentral interactions and interactions between second neighbors, and a discussion of the properties of crystals in which both ions are polarizable.

2.1 Theory of Vibrations of a Lattice of Point Ions

Since the present work is an extension of Kellermann's,[15] we begin with a brief summary of his treatment of the problem, at the same time explaining our own notation. We shall find Figs. 1(a) and 1(b) useful in defining certain terms. In Kellermann's approximation the atoms are regarded as exerting short-range "overlap" forces between nearest neighbors only, with Coulomb interactions between ions throughout the crystal. The polarizability of the ions is neglected. The force between nearest neighbors is taken to be a central force, so that the energy per unit cell is given by

$$U_0=-\alpha_M\frac{Z^2e^2}{r_0}+6\Phi^{(R)}(r_0), \tag{2.1.1}$$

where α_M is the Madelung constant, $2r_0$ the side of the (cubic) unit cell and Ze the charge on the positive ion ($e=+4.803\times10^{-10}$ esu). Two parameters A and B are defined in terms of the derivatives of the overlap potential $\Phi^{(R)}$ by

$$\frac{1}{r_0}\left[\frac{d}{dr}\Phi^{(R)}\right]_{r=r_0}=\frac{e^2B}{2v},$$
$$\text{and} \tag{2.1.2}$$
$$\left[\frac{d^2}{dr^2}\Phi^{(R)}\right]_{r=r_0}=\frac{e^2A}{2v},$$

where $v=2r_0^3$ is the volume of the (trigonal) unit cell. The appearance of $e^2/2v$ in these definitions is merely a convention which makes A and B of a convenient order of magnitude. Kellermann takes $Z=1$ throughout his work. We use the superscript (R) to distinguish quantities associated with the repulsive interaction between ions from those associated with Coulomb interaction, for which we use the superscript (C). Kellermann shows that for the static lattice to be in equilibrium,

$$B=-\tfrac{2}{3}\alpha_MZ^2=-1.165Z^2,$$

and that the elastic constants are given by the expressions

$$c_{11}=\frac{e^2}{4r_0^4}A-2.56\frac{(Ze)^2}{2r_0^4},$$
$$c_{12}=\frac{e^2}{4r_0^4}B+1.28\frac{(Ze)^2}{2r_0^4}, \tag{2.1.3}$$
$$c_{44}=0.696(Ze)^2/2r_0^4,$$

and the compressibility β by

$$\frac{1}{\beta}=\frac{c_{11}+2c_{12}}{3}=\frac{e^2}{12r_0^4}(A+2B).$$

In general a force constant between atoms of type κ and κ' in unit cells l and l' will be written as

$$\frac{\partial^2}{\partial x\partial y}\Phi(l\kappa,l'\kappa')\equiv\Phi_{xy}(l\kappa,l'\kappa')$$
$$=\Phi_{xy}^{(R)}(l\kappa,l'\kappa')+z^2\Phi_{xy}^{(C)}(l\kappa,l'\kappa').$$

$\Phi_{xy}^{(R)}(l\kappa,l'\kappa')$ will usually be zero unless the atoms are nearest neighbors. If we take $\kappa=1$ to denote the positive

ion, and label the unit cells as shown in Fig. 1(a), it follows from these definitions that

$$\Phi_{xx}{}^{(R)}(01,02)=\Phi_{yy}{}^{(R)}(01,12)=\text{etc.}=e^2B/2v,$$

and (2.1.4)

$$\Phi_{zz}{}^{(R)}(01,02)=\Phi_{xx}{}^{(R)}(01,12)=\text{etc.}=e^2A/2v.$$

Other force constants such as $\Phi_{xy}{}^{(R)}(01,02)$ are identically zero.

In a lattice vibration, the displacement $\mathbf{u}(l\kappa)$ of an atom from its equilibrium position $\mathbf{r}(l\kappa)$, due to a normal mode of wave vector $\mathbf{q}(q=2\pi/\lambda)$ and circular frequency ω is given by

$$\mathbf{u}(l\kappa)=\mathbf{U}(\kappa)\exp i(\mathbf{q}\cdot\mathbf{r}(l\kappa)-\omega t). \quad (2.1.5)$$

The direction of $\mathbf{U}$ specifies the polarization of the mode (note that polarization frequently occurs with another meaning). We now define quantities to which we shall refer as *coefficients*,

$$R_{xy}(\kappa\kappa')=-\sum_{l'}\Phi_{xy}{}^{(R)}(l\kappa,l'\kappa')\times\exp\{i\mathbf{q}\cdot[\mathbf{r}(l'\kappa')-\mathbf{r}(l\kappa)]\},$$

and (2.1.6)

$$C_{xy}(\kappa\kappa')=-\sum_{l'}\Phi_{xy}{}^{(C)}(l\kappa,l'\kappa')\times\exp\{i\mathbf{q}\cdot[\mathbf{r}(l'\kappa')-\mathbf{r}(l\kappa)]\}.$$

Their sum, which is similarly related to $\Phi_{xy}(l\kappa,l'\kappa')$, is given by

$$M_{xy}(\kappa\kappa')=R_{xy}(\kappa\kappa')+Z^2C_{xy}(\kappa\kappa').$$

The coefficients $R_{xy}(\kappa\kappa')$ are fully determined by the parameters A and B, for example,

$$R_{xx}(12)=-(e^2/v)[A\cos q_xr_0+B(\cos q_yr_0+\cos q_zr_0)], \quad (2.1.7)$$

when only nearest neighbors interact. From their definition in terms of the electrostatic potential, it follows that

$$C_{xy}(11)=-e^2\lim_{\mathbf{r}\to0}\left[\sum_l{}'\frac{\partial^2}{\partial x\partial y}\left(\frac{1}{|\mathbf{r}-\mathbf{r}_l|}\right)\exp i\mathbf{q}\cdot\mathbf{r}_l\right],$$

and

$$C_{xy}(12)=e^2\exp i\mathbf{q}\cdot[\mathbf{r}(2)-\mathbf{r}(1)]\times\lim_{\mathbf{r}\to\mathbf{r}(1)-\mathbf{r}(2)}\left[\sum_l\frac{\partial^2}{\partial x\partial y}\left(\frac{1}{|\mathbf{r}-\mathbf{r}_l|}\right)\exp i\mathbf{q}\cdot\mathbf{r}_l\right].$$

In these expressions $\mathbf{r}_l$ denotes a lattice translation and, for a sodium chloride type of structure, $r(1)=0$, $r(2)=(r_0,0,0)$. These quantities were evaluated by Kellermann using the Ewald method, and have been tabulated for 48 positions of $\mathbf{q}$ in the unique volume of the Brillouin zone. It is more convenient in this case to use corresponding dimensionless functions of $\mathbf{q}$, given by

$$(C_1)_{xy}=(v/e^2)C_{xy}(11),$$

and (2.1.8)

$$(C_2)_{xy}=-(v/e^2)C_{xy}(12).$$

$(C_1)_{xx}$ and $(C_2)_{xx}$ then tend to the same value at $q=0$. The fact that $(C_1)_{xx}$ and $(C_1)_{yy}$ tend to different values as $q\to0$, $+8\pi/3$ and $-4\pi/3$, respectively, for $\mathbf{q}$ along [100] is well known.[13,15]

The equations of motion of the ions lead to the set of equations

$$\sum_{\kappa'y}[M_{xy}(\kappa\kappa')-m_\kappa\omega^2\delta_{xy}\delta_{\kappa\kappa'}]U_y(\kappa')=0, \quad (2.1.9)$$

and the condition for the solubility of this set of equations then gives a determinantal relation for $\omega(\mathbf{q})$,

$$|M-Im\omega^2|=0, \quad (2.1.10)$$

where I is the unit matrix of order six, and the elements of the matrix M are the coefficients $M_{xy}(\kappa\kappa')$. For the type of lattice we are considering, where every ion is on a center of symmetry, $M_{xy}(12)=M_{yx}(21)$, and, if only nearest neighbors interact and the ions are not polarizable, $M_{xy}(11)=M_{xy}(22)$.

Kellermann's theory accounts quite well for the measured elastic constants and the infrared absorption frequency of sodium chloride, and leads to a frequency distribution of the normal modes which explains quantitatively the variation of Θ_D with temperature. The theory is, however, inconsistent with the dielectric properties of the alkali halides, since the polarizability of the ions is neglected. Lyddane and Herzfeld[13] had shown, prior to Kellermann's work, that when this is taken into account, there is wide disagreement between the calculated and measured values of the infrared absorption frequency, and indeed the lattice should be unstable against certain vibration modes (see later). They attributed this to their neglect of the fact that the short-range interaction between ions is dependent on the state of polarization of these ions, and vice versa. The theory given in subsequent sections takes this factor into account.

2.2 General Theory with Polarizable Ions

The connection between the polarization of ions and the repulsive force between them has recently been considered by Yamashita and Kurosawa,[21] by Dick and Overhauser,[18] and by Hanlon and Lawson.[19] These latter authors[18,19] have independently suggested a "shell model" for an ion having a closed electron configuration. Their models are somewhat different, particularly as to the charge in the shell, which represents the outer electrons. We have used this model with certain extensions in an attempt to give an improved theory of the

[21] J. Yamashita and J. Kurosawa, J. Phys. Soc. Japan **10**, 610 (1955).

lattice dynamics of ionic crystals. A simple version of the theory which applies when only the negative ion is polarizable is found to be in fairly good agreement with our experimental results for sodium iodide. The general treatment is applicable to any diatomic cubic crystal in which the surroundings of each ion have tetrahedral symmetry,[16] and therefore includes NaCl, CsCl, ZnS, and isomorphous structures. The theory remains within the framework of the Born-von Kármán theory; in particular both the harmonic and the adiabatic approximations are utilized. In the Born-von Kármán theory the energy perturbation in the lattice is written

$$\Phi_2=-\tfrac{1}{2}\sum_{\kappa\kappa'}\sum_{ll'}\sum_{xy}\Phi_{xy}(l\kappa,l'\kappa')u_x(l\kappa)u_y(l'\kappa'), \quad (2.2.1)$$

where for an alkali halide κ assumes the values 1 and 2. The equations of motion

$$m_\kappa\ddot{u}x(l\kappa)=-\partial\Phi_2/\partial u_x(l\kappa),$$

then lead to Eqs. (2.1.9). The summation (2.2.1) is now extended over four values of κ, $\kappa=3$ denoting the shell of the positive ion, $\kappa=4$ that of the negative ion while indices 1 and 2 refer to the corresponding cores. The charge in a particular unit κ (core or shell) is taken as X_1e, X_2e, Y_1e, Y_2e, for $\kappa=1$, 2, 3, and 4, respectively. The charge on the positive ion is then $Z_1e=(X_1+Y_1)e$, and on the negative ion, $Z_2e=(X_2+Y_2)e$, while $Z_1+Z_2=0$.

The force constants coupling a shell isotropically to the core of the same atom are denoted by k_1 and k_2 for the positive and negative ions, respectively. The polarizability of a free negative ion is then $Y_2^2e^2/k_2$; we shall find, however, that its value is reduced in the crystal. Separate symbols for the short-range force constants are introduced as follows:

$\Phi_{xy}^{(S)}(l3,l'4)$, between the shells,

$\Phi_{xy}^{(D)}(l1,l'2)$, between the cores,

$\Phi_{xy}^{(F)}(l1,l'4)$, core of positive to shell of negative ion,

$\Phi_{xy}^{(F)}(l3,l'2)$, shell of positive to core of negative ion.

Although it is not dictated by the physics of the problem, we propose to assume that the two latter force constants are equal. This makes the interaction between two ions completely symmetrical and simplifies the analysis, besides being physically not unreasonable. There are coefficients corresponding to the various force constants [Eq. (2.1.6)]. For example,

$$S_{xy}(34)=-\sum_{l'}\Phi_{xy}^{(S)}(l3,l'4)\times\exp i\mathbf{q}\cdot[\mathbf{r}(l'2)-\mathbf{r}(l1)]. \quad (2.2.2)$$

In this definition use has been made of the fact that $\mathbf{r}(l2)=\mathbf{r}(l4)$ and $\mathbf{r}(l1)=\mathbf{r}(l3)$. $D_{xy}(12)$ and $F_{xy}(14)=F_{xy}(32)$ are similarly defined in terms of the appropriate force constants. $S_{xx}(34)$ for example will be given by an expression similar to Eq. (2.1.7), although not necessarily involving the same parameters A and B as appear there.

The matrix M of Eq. (2.1.10) is of order six for a cubic diatomic crystal. Use of a shell model with both ions polarizable raises the order to twelve. Fortunately however, when $\mathbf{q}$ is in one of the directions [100], [110], or [111] the set of Eq. (2.1.9) can be reduced to three separate sets, [or in other words the determinant (2.1.10) factors], each of which determines $\omega(\mathbf{q})$ for a single mode, for which the polarization is fixed by the space-group symmetry of the crystal. For example, with $\mathbf{q}$ along [100], $U_y=U_z=0$ in Eq. (2.1.9) (for a longitudinal mode) and Eq. (2.1.9) reduces to

$$m_\kappa\omega^2U(\kappa)=\sum_{\kappa'}M(\kappa\kappa')U(\kappa'), \quad (2.2.3)$$

where in this case $M(\kappa\kappa')=M_{xx}(\kappa\kappa')$. A similar expression applies whenever the direction of $\mathbf{U}$ is fixed by symmetry, and, in general, $M(\kappa\kappa')$ of Eq. (2.2.3) is a linear combination of $M_{xx}(\kappa\kappa')$, $M_{xy}(\kappa\kappa')$, etc. Symbols such as $M(\kappa\kappa')$, $R(\kappa\kappa')$ without the suffixes will always denote such a linear combination. Explicit formulas, for the three possible directions of $\mathbf{q}$ are given in Table I. It follows that when $\mathbf{q}$ is in a symmetry direction the matrix M is only of order four even when both ions are polarizable.

Equations (2.2.3) must be invariant under a uniform translation of the crystal, that is, there must be a solution with $\omega=0$ corresponding to $U(1)=U(2)=U(3)=U(4)$. Hence $\{\sum_{\kappa'}M(\kappa\kappa')\}_{q=0}=0$. Use of this fact together with previous definitions gives

$$\begin{aligned}
M(11)&=k_1+D(11)+F(11)+X_1^2C(11),\\
M(12)&=D(12)-X_1X_2C(12),\\
M(13)&=-k_1+X_1Y_1C(11),\\
M(14)&=F(14)-X_1Y_2C(12),\\
M(22)&=k_2+D(22)+F(22)+X_2^2C(11),\\
M(23)&=F^*(32)-X_2Y_1C^*(12),\\
M(24)&=-k_2+X_2Y_2C(11),\\
M(33)&=k_1+S(33)+F(33)+Y_1^2C(11),\\
M(34)&=S(34)-Y_1Y_2C(12),\\
M(44)&=k_2+S(44)+F(44)+Y_2^2C(11).
\end{aligned}$$

TABLE I. Explicit expressions for the matrix elements $M(\kappa\kappa')$ for modes in the symmetry directions derived following Kellermann.[a]

Mode ($\mathbf{q}$)	Polarization	$M(\kappa\kappa')$
$L[100]$	[100]	$M_{xx}(\kappa\kappa')$
$T[100]$	[010] etc.	$M_{yy}(\kappa\kappa')$
$L[111]$	[111]	$M_{xx}(\kappa\kappa')+2M_{xy}(\kappa\kappa')$
$T[111]$	[$\bar{1}$12] etc.	$M_{xx}(\kappa\kappa')-M_{xy}(\kappa\kappa')$
$L[110]$	[110]	$M_{xx}(\kappa\kappa')+M_{xy}(\kappa\kappa')$
$T_1[110]$	[001]	$M_{zz}(\kappa\kappa')$
$T_2[110]$	[$\bar{1}$10]	$M_{xx}(\kappa\kappa')-M_{xy}(\kappa\kappa')$

[a] See reference 15, pp. 540–542.

The remaining coefficients can be written down by using the fact that the matrix whose elements are the $M(\kappa\kappa')$ is Hermitian. The following conditions then hold

$$\{D(11)+D(12)\}_{q=0}=0,$$
$$\{S(33)+S(34)\}_{q=0}=0,$$
$$\{F(11)+F(14)\}_{q=0}=0,$$
$$\{C(11)+C(12)\}_{q=0}=0.$$

When only nearest neighbor atoms interact with short-range forces, as will be assumed in most of this work, $D(11)$, $S(33)$, etc., are constants, independent of $\mathbf{q}$, and the notation may then be simplified by writing

$$D\equiv D(12),$$
$$S\equiv S(13),$$
$$F\equiv F(14),$$

and

$$\begin{aligned}&D_0\equiv D(11)=D(22)=-(D)_{q=0},\\&S_0\equiv S(33)=S(44)=-(S)_{q=0},\\&F_0\equiv F(11)=F(22)=F(33)=F(44)=-(F)_{q=0}.\end{aligned}\tag{2.2.5}$$

Making use of the definitions of C_1 and of C_2 [Eq. (2.1.8)], Eqs. (2.2.3) written out in full become

$$\begin{aligned}m_1\omega^2U(1)=&[k_1+D_0+F_0+X_1^2(e^2/v)C_1]U(1)\\&+[D+X_1X_2(e^2/v)C_2]U(2)\\&+[-k_1+X_1Y_1(e^2/v)C_1]U(3)\\&+[F+X_1Y_2(e^2/v)C_2]U(4),\\m_2\omega^2U(2)=&[D^*+X_2X_1(e^2/v)C_2^*]U(1)\\&+[k_2+D_0+F_0+X_2^2(e^2/v)C_1]U(2)\\&+[F^*+X_2Y_1(e^2/v)C_2^*]U(3)\\&+[-k_2+X_2Y_2(e^2/v)C_1]U(4),\\m_3\omega^2U(3)=&[-k_1+Y_1X_1(e^2/v)C_1]U(1)\\&+[F+Y_1X_2(e^2/v)C_2]U(2)\\&+[k_1+S_0+F_0+Y_1^2(e^2/v)C_1]U(3)\\&+[S+Y_1Y_2(e^2/v)C_2]U(4),\\m_4\omega^2U(4)=&[F^*+Y_2X_1(e^2/v)C_2^*]U(1)\\&+[-k_2+Y_2X_2(e^2/v)C_1]U(2)\\&+[S^*+Y_2Y_1(e^2/v)C_2^*]U(3)\\&+[k_2+S_0+F_0+Y_2^2(e^2/v)C_1]U(4).\end{aligned}\tag{2.2.6}$$

We may now introduce the equivalent of the adiabatic approximation by setting $m_3=m_4=0$, so that the shells occupy positions of equilibrium *at each instant*. Using the third and fourth equations one may then eliminate $U(3)$ and $U(4)$ from the first and second equations, which then in principle provide a solution of the problem.

It is, however, both convenient and illuminating to express these equations first of all in terms of coordinates $U(1)$, $U(2)$, and $W(1)=U(3)-U(1)$, $W(2)=U(4)-U(2)$. These quantities are related to the dipole moments $p(l1)$ and $p(l2)$ by the equations

$$p(l1)=eY_1W(1)\exp i[\mathbf{q}\cdot\mathbf{r}(l1)-\omega t],$$

and similarly for $p(l2)$. We comment on the significance of this later. On adding together the first and third of Eqs. (2.2.6), and the second and fourth, and introducing $W(1)$ and $W(2)$, we obtain

$$\begin{aligned}m_1\omega^2U(1)=&[R_0+Z_1^2(e^2/v)C_1]U(1)\\&+[R+Z_1Z_2(e^2/v)C_2]U(2)\\&+[T_0+Z_1Y_1(e^2/v)C_1]W(1)\\&+[T+Z_1Y_2(e^2/v)C_2]W(2),\\m_2\omega^2U(2)=&[R^*+Z_2Z_1(e^2/v)C_2^*]U(1)\\&+[R_0+Z_2^2(e^2/v)C_1]U(2)\\&+[T^*+Z_2Y_1(e^2/v)C_2^*]W(1)\\&+[T_0+Z_2Y_2(e^2/v)C_1]W(2),\\0=&[T_0+Y_1Z_1(e^2/v)C_1]U(1)\\&+[T+Y_1Z_2(e^2/v)C_2]U(2)\\&+[T_0+k_1+Y_1^2(e^2/v)C_1]W(1)\\&+[S+Y_1Y_2(e^2/v)C_2]W(2),\\0=&[T^*+Y_2Z_2(e^2/v)C_2^*]U(1)\\&+[T_0+Y_2Z_2(e^2/v)C_1]U(2)\\&+[S^*+Y_2Y_1(e^2/v)C_2^*]W(1)\\&+[T_0+k_2+Y_2^2(e^2/v)C_1]W(2),\end{aligned}\tag{2.2.7}$$

where $R=D+S+2F$, and

$$T=S+F.\tag{2.2.8}$$

It will be noticed that Eqs. (2.2.7) are somewhat more symmetrical than Eqs. (2.2.6) from which they were derived. Equations (2.2.7) could, in fact, have been derived in another way, which consists in expressing the energy perturbation [Φ_2 of Eq. (2.2.1)] as a quadratic function of the nuclear displacements $\mathbf{u}(l\kappa)$ *and* the atomic dipole moments $\mathbf{p}(l\kappa)$. Tolpygo[22] and Mashkevich and Tolpygo[23] have given a wave-mechanical justification for this procedure, using the tight-binding approximation. Their analysis was not taken in a direction that would lead to Eqs. (2.2.7), however, and their expression for the energy perturbation does not include terms which correspond to the coefficient S in Eqs. (2.2.7). A theory resembling that of Mashkevich and Tolpygo in some respects has also been proposed by Yamashita and Kurosawa.[21] Equations (2.2.7) may be derived in a purely phenomenological way by *postulating* an expression for the energy perturbation Φ_2 of the form

[22] K. B. Tolpygo, J. Exptl. Theoret. Phys. (U.S.S.R.) **20**, 497 (1950).

[23] V. S. Mashkevich and K. B. Tolpygo, J. Exptl. Theoret. Phys. (U.S.S.R.) **32**, 520 (1957) [translation: Soviet Phys.—JETP **5**, 435 (1957)].

$$\Phi_2=-\tfrac{1}{2}\sum_{l\kappa x}\sum_{l'\kappa' y}\Big\{\Phi_{xy}{}^{(R)}(l\kappa,l'\kappa')u_x(l\kappa)u_y(l'\kappa')$$
$$+\Phi_{xy}{}^{(T)}(l\kappa,l'\kappa')\Big[\frac{u_x(l\kappa)p_y(l'\kappa')}{Y_{\kappa'}e}+\frac{p_x(l\kappa)u_y(l'\kappa')}{Y_\kappa e}\Big]$$
$$+\frac{1}{Y_\kappa Y_{\kappa'}e^2}\Phi_{xy}{}^{(S)}(l\kappa,l'\kappa')p_x(l\kappa)p_y(l'\kappa')\Big\}$$
$$+\tfrac{1}{2}\sum_{l\kappa x}\Big\{\frac{1}{\alpha_\kappa}p_x{}^2(l\kappa)$$
$$-[p_x(l\kappa)+Z_\kappa e u_x(l\kappa)]E_x(l\kappa)\Big\}. \quad (2.2.9)$$

Here $\mathbf{E}(l\kappa)$ is the effective field at $\mathbf{r}(l\kappa)$ and α_κ is the polarizability that an atom of type κ would have in the absence of short-range interaction between the dipoles (that is, when $\Phi_{xy}{}^{(S)}=0$). The actual polarizability of the atom in the crystal is not quite the same as α_κ. Further discussion of this point will be found in Appendix 3. The constants Y_κ are now to be regarded simply as normalizing factors;when they are equal they could be incorporated in the "generalized force constants" $\Phi_{xy}{}^{(T)}$ and $\Phi_{xy}{}^{(S)}$ to give an expression completely symmetrical in u and in p, the coordinates and dipole moments. Use of the expression (2.2.9) with the equations of motion given by Mashkevich and Tolpygo[23]

$$m_\kappa \ddot{u}_x(l\kappa)=-\frac{\partial\Phi_2}{\partial u_x(l\kappa)}, \quad 0=\frac{\partial\Phi_2}{\partial p_x(l\kappa)}$$

leads eventually to Eqs. (2.2.7).

However derived, Eqs. (2.2.7) provide in principle a solution of the problem, for on elimination of $W(1)$ and $W(2)$ we obtain two equations which may be written

$$\begin{aligned}m_1\omega^2U(1)&=A(11)U(1)+A(12)U(2),\\ m_2\omega^2U(2)&=A^*(12)U(1)+A(22)U(2),\end{aligned} \quad (2.2.10)$$

leading to the characteristic equation

$$\begin{vmatrix}A(11)-m_1\omega^2 & A(12)\\ A^*(12) & A(22)-m_2\omega^2\end{vmatrix}=0, \quad (2.2.11)$$

as the condition for solubility. If the analysis is extended to include short-range interaction between other than nearest neighbors, the form of Eq. (2.2.7) is unchanged, except that coefficients such as R_0 are not constants, but must be replaced by $R(11)$ and $R(22)$ which are functions of $\mathbf{q}$.

2.3 Negative Ion Polarizable

The general result obtained for the elements $A(11)$, etc., of Eq. (2.2.11) by eliminating $W(1)$ and $W(2)$ from Eqs. (2.2.7), is very cumbersome, and we shall consider only certain special cases in detail, the first, which is applicable to sodium iodide, being the situation when only the negative ion is polarizable. In this case $k_1=\infty$, $k_2=k$, and $Y_2=Y$. Since the short-range interaction can be described in terms of two coefficients, involving force constants between the positive ion and the shell of the negative ion, and between the positive ion and the core of the negative ion, we may set $F=0$ and retain only S and D. When each ion is on a center of symmetry, as in an alkali halide, we have $A(12)=A(21)=A^*(12)$. The polarizability of the negative ion is given by

$$\alpha=\frac{Y^2e^2}{k+S_0}, \quad (2.3.1)$$

where

$$\frac{4\pi\alpha}{3v}=\frac{\epsilon-1}{\epsilon+2}.$$

It is then found that

$$\begin{aligned}A(11)&=R_0-\frac{S^2}{f(k+S_0)}\\ &\quad+\frac{Z^2e^2}{fv}\Big[C_1-\frac{2SYC_2}{(k+S_0)Z}+\frac{\alpha}{v}(C_1{}^2-C_2{}^2)\Big],\\ A(12)&=A(21)=R-\frac{SS_0}{f(k+S_0)}\\ &\quad+\frac{Z^2e^2}{fv}\Big[-C_2+\frac{Y(C_1S-C_2S_0)}{(k+S_0)Z}\Big],\\ A(22)&=R_0-\frac{S_0{}^2}{f(k+S_0)}\\ &\quad+\frac{Z^2e^2}{fv}\Big\{C_1\Big[1+\frac{2S_0Y}{(k+S_0)Z}\Big]\Big\}.\end{aligned} \quad (2.3.2)$$

Here f is simply a convenient abbreviation for $1+(\alpha/v)C_1$. If $k\to\infty$ these results become

$$\begin{aligned}A(11)&=A(22)=R_0+Z^2e^2C_1/v,\\ A(12)&=A(21)=R-Z^2e^2C_2/v,\end{aligned}$$

which are just the expressions for the point ion model and are identical with those results of Kellermann which apply when $\mathbf{q}$ is in a symmetry direction. In particular the coefficient R, which from Eq. (2.2.8) appears here as $D+S$, is seen to be identical with the coefficient R defined in Sec. 2.1. In other words $D+S$, as might be expected, is the coefficient of the interaction of the ions when they behave as rigid units. Returning to Eqs. (2.3.2) we introduce a parameter

$$d=-S_0Y/(k+S_0). \quad (2.3.3)$$

This quantity is positive, since Y is negative. It is a measure of the polarizability of the negative ion under

the action of the short-range forces. Equations (2.3.2) may then be written

$$A(11)=R_0-\frac{S^2e^2d^2}{S_0^2\alpha f}+\frac{e^2}{vf}\left[Z^2C_1+2ZC_2d\frac{S}{S_0}+\frac{Z^2\alpha}{v}(C_1^2-C_2^2)\right],$$

$$A(12)=R-\frac{Se^2d^2}{S_0\alpha f}+\frac{e^2}{vf}\left[-Z^2C_2+dZ\left(C_2-C_1\frac{S}{S_0}\right)\right], \quad (2.3.4)$$

$$A(22)=R_0-\frac{e^2d^2}{\alpha f}+\frac{e^2}{vf}[ZC_1(Z-2d)].$$

We note that S is involved only in the sum $R=D+S$, and in the ratio S/S_0, from which it follows that the experimental results will not enable us to determine D and S separately, that is, we cannot deduce what proportion of the overlap force acts through the shell. If we assume that this force acts entirely through the shell, then $D=0$ and an experimental determination of the values of $R_0=S_0$, d and α will give values for Y and k.

When $q=0$ we have $S=-S_0$, $D=-D_0$ [Eqs. (2.2.5)] and $C_1=C_2$. It follows that $A(11)=A(22)=-A(12)$, when $q=0$. There is then a solution of Eq. (2.2.11),

$$(\mu\omega^2)_{q=0}=R_0-\frac{e^2d^2}{\alpha}+\frac{e^2}{v}\left[\frac{C_1(Z-d)^2}{1+\alpha C_1/V}\right], \quad (2.3.5)$$

where the reduced mass $\mu=m_1m_2/(m_1+m_2)$. The frequency of the transverse optic mode, ω_T, may be obtained by setting $C_1=-4\pi/3$ and that of the longitudinal mode, ω_L, by setting $C_1=+8\pi/3$. From Eq. (2.3.1) we have, however, that

$$\left(1-\frac{4\pi\alpha}{3v}\right)^{-1}=\frac{\epsilon+2}{3} \quad \text{and} \quad \left(1+\frac{8\pi\alpha}{3v}\right)^{-1}=\frac{\epsilon+2}{3\epsilon},$$

so that

$$(\mu\omega_T^2)_{q=0}=\left(R_0-\frac{e^2d^2}{\alpha}\right)-\frac{4\pi e^2(Z-d)^2(\epsilon+2)}{9v}, \quad (2.3.6)$$

and

$$(\mu\omega_L^2)_{q=0}=\left(R_0-\frac{e^2d^2}{\alpha}\right)+\frac{8\pi e^2(Z-d)^2(\epsilon+2)}{9v\epsilon}. \quad (2.3.7)$$

When the positive and the negative ions are relatively displaced, as rigid units, by an amount $\mathbf{u}$, the overlap force acting on each is $(D_0+S_0)\mathbf{u}=R_0\mathbf{u}$. From Eqs. (2.3.6) and (2.3.7) we see that use of a shell model for the negative ion replaces R_0 by an "effective coefficient" $R_0'=R_0-e^2d^2/\alpha$ and replaces the ionic charge Ze by an "effective charge" $Z'e=(Z-d)e$. In this last respect our result agrees with that of Born and Huang.[16]

It is of some interest to show that these equations are consistent with the general[24] equation $\epsilon_0/\epsilon=(\omega_L^2/\omega_T^2)_{q=0}$. Returning to Eq. (2.3.5) and introducing R_0' and Z' we obtain

$$\left(\frac{\omega_L^2}{\omega_T^2}\right)_{q=0}=\frac{R_0'+(8\pi/3v)(Z'e)^2/(1+8\pi\alpha/3v)}{R_0'-(4\pi/3v)(Z'e)^2/(1-4\pi\alpha/3v)}. \quad (2.3.8)$$

If we now define

$$\alpha_I=(Z'e)^2/R_0'=(Z-d)^2e^2/(R_0-e^2d^2/\alpha), \quad (2.3.9)$$

this result becomes

$$\left(\frac{\omega_L^2}{\omega_T^2}\right)_{q=0}=\frac{1+(8\pi/3v)(\alpha+\alpha_I)}{1-(4\pi/3v)(\alpha+\alpha_I)}\times\frac{1-4\pi\alpha/3v}{1+8\pi\alpha/3v}. \quad (2.3.10)$$

If we now consider the state of equilibrium of a system of cores and shells in an electric field, applied in such a way that there is no depolarizing field, we find that the ratio of polarization P to *effective* field E is

$$\frac{P}{E}=\frac{1}{v}\left[\frac{(Ye)^2}{k+S_0}+\frac{(Z'e)^2}{R_0'}\right]=\frac{\alpha+\alpha_I}{v}. \quad (2.3.11)$$

If the applied field is of such high frequency that the cores do not move, the term α_I does not appear. This enables us to identify α and α_I, respectively, as the electronic polarizability of the negative ion, and the ionic polarizability of the contents of one unit cell. The electronic polarizability is related to the high-frequency dielectric constant ϵ by

$$\frac{4\pi\alpha}{3v}=\frac{\epsilon-1}{\epsilon+2}, \quad (2.3.12)$$

while the static dielectric constant ϵ_0 is similarly related to the total polarizability, that is

$$\frac{4\pi(\alpha+\alpha_I)}{3v}=\frac{\epsilon_0-1}{\epsilon_0+2}. \quad (2.3.13)$$

When these results are used to eliminate α and α_I from Eq. (2.3.10), the equation reduces to $\omega_L^2/\omega_T^2=\epsilon_0/\epsilon$. When both ions are polarizable the derivation is more cumbersome, but the same final result is obtained.

2.4 Calculations of Dispersion Curves

We have computed dispersion curves for NaI in the three symmetric directions [100], [111], and [110], on the basis of the two models previously discussed—the point ion model, and the shell model with one ion only

[24] R. H. Lyddane, R. G. Sachs, and E. Teller, Phys. Rev. **59**, 673 (1941).

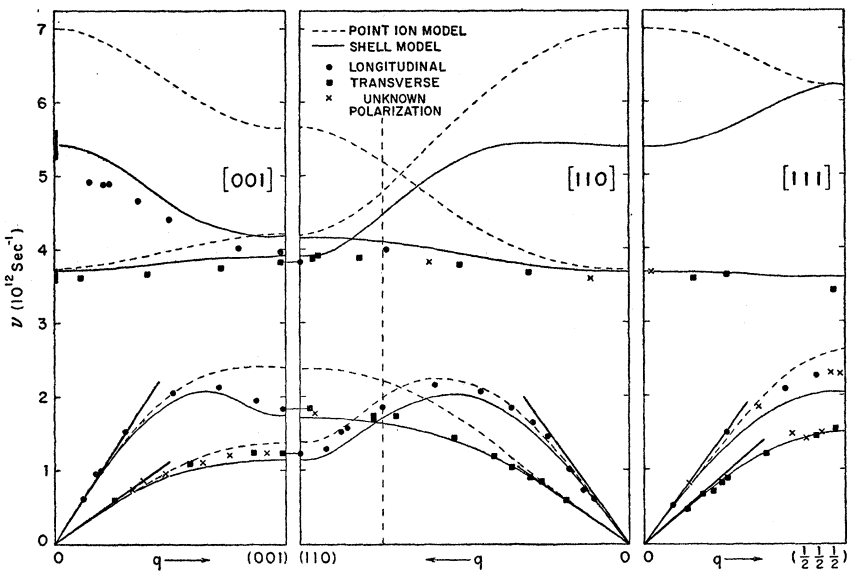

FIG. 2. The dispersion relations for sodium iodide in the [001], [110], and [111] directions. The points were determined by experiment at 110°K. Some points in the [001] direction are not independent of corresponding points in the [110] direction. Such points have been joined by a thin horizontal line. The solid curves have been calculated from the shell model and the dashed curves from the point ion model. These curves coincide for the transverse branches in the [111] direction. The slopes of the heavy solid lines indicate the appropriate velocities of sound as calculated from the elastic constants. The thick vertical bars represent the uncertainties in $(\nu_{TO})_{q=0}$ and $(\nu_{LO})_{q=0}$ deduced from existing knowledge of ω_0, ϵ, and ϵ_0.

polarizable, and forces acting through the shell. The calculated curves are shown in Fig. 2 together with experimental points to be discussed later. In the calculations on the point ion model the single disposable parameter was fixed by means of the elastic constant c_{11}. In the calculations on the shell model the three disposable parameters, selected to be $R_0=S_0$, d, and α/v, were fixed by means of c_{11} and the high- and low-frequency dielectric constants, ϵ and ϵ_0, by using Eqs. (2.1.3), (2.3.12), and (2.3.13). (In addition the experimental value of the lattice constant $2r_0$ was used.) The values used are shown in Table II. The value taken for c_{11} when the computations were carried out was slightly smaller than the best value now obtainable, based on the measurements of Dalven and Garland.[25] The dielectric constants were taken from a compilation by Born and Huang.[16] In Table III the elastic constants, dielectric constants, and infrared absorption frequency, $(\omega_T)_{q=0}$,[16] as measured and as computed on the shell model, are compared. The differences in the values of $(\omega_T)_{q=0}$ are compatible with the changes with temperature found experimentally for NaCl and KCl.[26]

TABLE II. Values of constants used in calculations on the shell model for NaI.

$r_0=3.21$ A
$v=2r_0^3=66.0$ A^3
$R_0=S_0=(e^2/v)(A+2B)=3.22\times10^4$ dyne/cm
$d=-S_0Y/(k+S_0)=0.31$
$\alpha/v=Y^2e^2/(k+S_0)v=0.093$
From these are found
$k=25.5\times10^4$ dyne/cm
$|Y|=2.76$ electrons in shell
and
the "effective charge" $Z(1-d)=0.69$

[25] R. Dalven and C. W. Garland, J. Chem. Phys. **30**, 346 (1959).
[26] M. Hass, Bull. Am. Phys. Soc. 4, 142 (1959).

As a matter of interest we also computed the dispersion curves in the [100] direction for the case in which field polarizability is included, but distortion polarizability is not taken into account. The results (Fig. 3) show the instability already mentioned in Sec. 2.1, that is, some of the acoustic frequencies become imaginary.

3. NEUTRON SCATTERING THEORY

3.1 Coherent Scattering

The differential cross section per primitive unit cell for scattering by phonons of the jth branch into one neutron group satisfying Eq. (1.1.1) can be written as[5,27]

$$\sigma_j(\mathbf{k}_0\rightarrow\mathbf{k}')=\frac{\hbar}{4\pi}\frac{k'}{k_0}\left\{\begin{matrix}N_j\\N_j+1\end{matrix}\right\}e^{-2W}\frac{g_j^2}{|J_j|}. \quad (3.1.1)$$

For phonon annihilation (neutron gain of energy) $N_j=[\exp(h\nu/k_BT)-1]^{-1}$ is used; for phonon creation

TABLE III. Comparison of experimental elastic and dielectric constants, and infrared frequencies, with those calculated on the shell model. The elastic constants are in units of 10^{12} dyne/cm^2.

	Experimental	Calculated
c_{11}	0.359[a]	0.3504[b]
c_{12}	0.075[a]	0.0758
c_{44}	0.0768[a]	0.0758
ϵ	2.91	2.91[b]
ϵ_0(R.T.)	6.60	...
ϵ_0(110°K)	6.18 (est.)	6.18[b]
ω_T(110°K)	...	2.31×10^{13}
ω_T(R.T.)	2.20×10^{13}	...

[a] Extrapolated to 110°K from data of Dalven and Garland (reference 24) measured in range 180°K to 300°K.
[b] Values used to fix disposable constants.

[27] I. Waller and P. O. Froman, Arkiv Fysik 4, 183 (1952).

(neutron loss of energy) N_j+1 is used. The geometrical factor

$$J_j=1+(\epsilon h/2E')[\mathbf{k}'\cdot\mathrm{grad}_q\nu_j], \qquad (3.1.2)$$

where $\epsilon=+1$, -1 for neutron energy loss or gain, respectively, sums over the number of normal modes contributing to one neutron group. In the notation of Sec. 2 the structure factor g_j for inelastic scattering (with $\mathbf{q}$ in the symmetry direction) is given by

$$g_j^2(\mathbf{q},\tau)=\frac{(\xi_j\cdot\mathbf{Q})^2}{\nu_j}\frac{b_2^2}{m_2}\frac{[b_1/b_2\pm U_j(2)/U_j(1)]^2}{m_1/m_2+[U_j(2)/U_j(1)]^2}, \qquad (3.1.3)$$

where b_1 and b_2 are the bound coherent scattering amplitudes of the two types of atoms, m_1 and m_2 are the masses of the two atoms, and ξ_j is a unit vector in the direction of polarization of the waves. The plus sign is used for even τ points and the minus sign for odd. [The Debye-Waller factor e^{-2W} has been assumed to be the same for the two types of atoms. If the two atoms have different Debye-Waller factors the ratio $b_1e^{-W_1}/b_2e^{-W_2}$ appears in the bracket in Eq. (3.1.3) instead of b_1/b_2 and e^{-2W_2} appears in Eq. (3.1.1).]

The reciprocal lattice is body-centered cubic. Figure 4 shows the $(1\bar{1}0)$ plane of the reciprocal lattice, each point being surrounded by its zone. The structure factor Eq. (3.1.3) repeats over the larger unit shown by bold lines. The structure factor has been computed for the symmetric directions in sodium iodide, using the two models of Sec. 2. The values taken for the scattering amplitudes were[28] $b_1=0.35$ for sodium, and $b_2=0.52$ for iodine. The quantities g_j^2 are plotted in Fig. 5 in units of $(b_2\xi\cdot\mathbf{Q})^2/m_2\nu$.

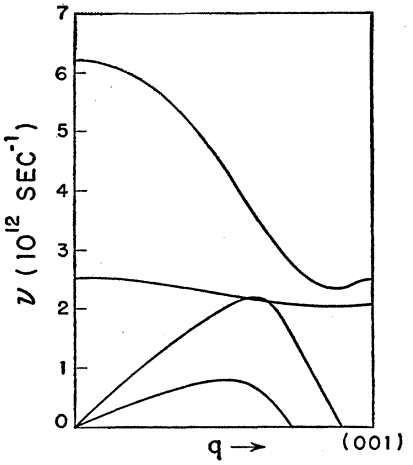

FIG. 3. The dispersion relations for the [001] direction calculated from the model of Lyddane and Herzfeld in which the polarization depends only on the electric field and not on the distortion of the ions. The parameters used in this calculation were the same as those used for the shell and point ion models except that $d=0$.

[28] *Neutron Cross Sections*, compiled by D. J. Hughes and R. B. Schwartz, Brookhaven National Laboratory Report BNL-325 (Superintendent of Documents, U. S. Government Printing Office, Washington, D. C., 1958), 2nd ed.

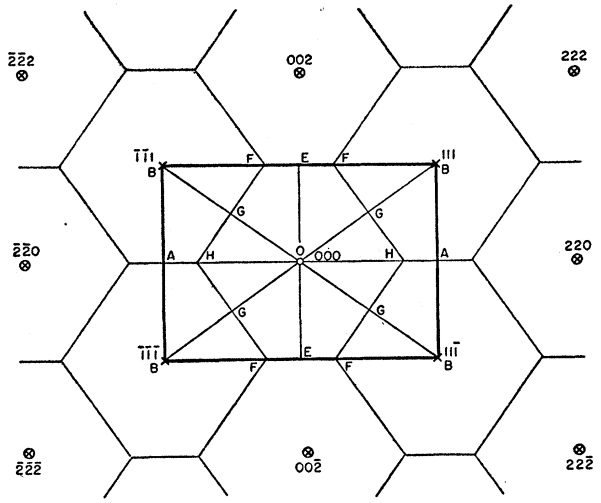

FIG. 4. $(1\bar{1}0)$ plane of the reciprocal lattice of NaI, each lattice point surrounded by its zone. The rectangular figure *BABEBABEB* is the unit over which the structure factor repeats.

3.2 Incoherent Scattering

It can happen that there is an ambiguity in the scattering amplitude (b_κ) at a particular lattice site (κ) because of the occurrence of different neutron-nuclear spin states, or that there are ambiguities in the scattering amplitude, atomic mass (m_κ), or wave amplitude $U(\kappa)$ at the site because of the presence of different isotopes on the site. Fluctuations in the masses and wave amplitudes due to isotopes cannot be taken into account accurately, because they give rise to effects on the normal modes themselves of the same order as the effects on neutron scattering. The ambiguity in the scattering amplitude can be taken into account, however, and gives rise to an incoherent scattering.

The incoherent cross section of the atoms on sites of type κ is defined in the usual way as

$$\sigma_{\mathrm{inc}}(\kappa)=4\pi(\langle b^2\rangle-\langle b\rangle^2). \qquad (3.2.1)$$

In general the incoherent scattering can be calculated in terms of these cross sections for a crystal with more than one atom per unit cell, only if the frequencies, *and wave amplitudes* of all the normal modes are known, a formidable requirement. In this paper however, we are interested largely in computing the incoherent scattering due to the very flat transverse optical modes, which appears in the energy distributions as a neutron group, and which can be confused with the coherent scattering.

For the particular case of sodium iodide the ratio of the masses of iodine to sodium $m_2/m_1=5.5$. The calculations of Sec. 2 showed that, for all the optical branches in the symmetry directions, the ratio of the wave amplitudes $U(2)/U(1)\leq m_1/m_2\approx 0.18$. In the optical modes therefore essentially only the light atoms move. Since

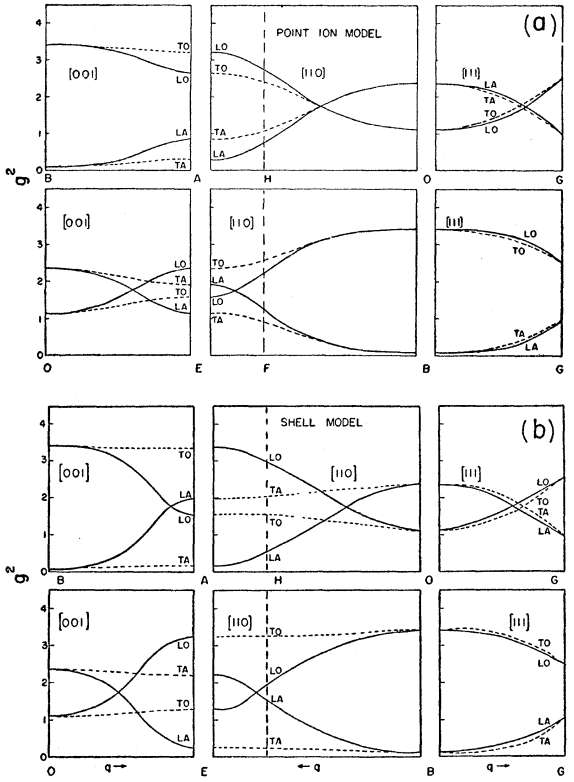

FIG. 5. Calculated structure factors, g^2, for (a) the point ion model, and (b) the shell model, in units of $b_2(\xi\cdot\mathbf{Q})^2/m_2\nu$ for the three symmetric directions in the Brillouin zone. The capital letters refer to the positions in the reciprocal lattice shown in Fig. 4.

the sodium atoms are on a cubic lattice, the theorems of Placzek and Van Hove[11] on the incoherent scattering by a monatomic cubic lattice apply. The ratio of incoherent to coherent scattering for the transverse optical modes is therefore

$$\frac{\sigma_{\rm inc}(\mathbf{k}_0\rightarrow\mathbf{k}')}{\sigma_{\rm coh}(\mathbf{k}_0\rightarrow\mathbf{k}')}\approx\frac{2}{3}\frac{Q^2\sigma_{\rm inc}({\rm Na})}{(\mathbf{Q}\cdot\xi)^2\sigma_{\rm coh}({\rm Na})} \qquad (3.2.2)$$

(We have used the facts that there are two TO modes per sodium atom and that $|J|\approx 1$ for the flat TO modes.) All other quantities are the same for coherent and incoherent scattering. This is slightly an overestimate in the case of NaI since scattering by the iodine does make a small contribution and is nearly all coherent. The cross sections for sodium are[28]: $\sigma_{\rm coh}=1.55$ b, $\sigma_{\rm inc}=1.8_5$ b. For the most favorable polarization therefore

$$\sigma_{\rm inc}(\mathbf{k}_0\rightarrow\mathbf{k}')/\sigma_{\rm coh}(\mathbf{k}_0\rightarrow\mathbf{k}')\approx 0.8.$$

4. THE EXPERIMENT

4.1 Experimental Methods

The experiment consisted in measuring the energy distributions of initially monoenergetic neutrons which were scattered from a single crystal of sodium iodide, using two different neutron spectrometers. All measurements were made with the $(1\bar{1}0)$ plane of the crystal horizontal.

The crystal was a 3.8-cm cube supplied by the Harshaw Chemical Company. Its faces were cut parallel to the {100} planes. The full widths at half maximum of the rocking curves of the {222} planes as measured in the parallel position against a (220) plane of a silicon crystal were about $1\frac{1}{4}$ deg.

The measurements were made with the crystal mounted in a metal cryostat. The specimen was cooled from above and was surrounded by a radiation shield in contact with liquid nitrogen. The temperature of the crystal was 110°K.

Some of the results were obtained at the Chalk River *NRX* reactor using a time of flight spectrometer[29] in which a pulsed beam of monochromatic neutrons was produced by Bragg reflection from {220} planes of an aluminum crystal spinning about its [111] axis. The wavelength was 1.54 A. Some of these neutrons were then scattered by the sodium iodide crystal into one of the three counters shown in Fig. 6. The times of flight of neutrons which entered the counters were measured directly from the time they left the spinning crystal to the time the count was recorded. The spectrometer was calibrated by subtracting the observed time of flight for neutrons which entered a counter mounted in the specimen position from the time of flight observed for the elastic peak when vanadium was in the specimen position. The values obtained by this method were checked against absolute measurements of appropriate lengths and angles, the agreement being within the experimental error in either calibration. The full width at half maximum of the vanadium peak represented a wavelength spread of about 0.045 A.

One of the features of this spectrometer was the use of three counters spaced 1.7 degrees apart. In the method of successive approximations (see below) one counter will not always yield a phonon in the desired direction, but the probability of obtaining such a

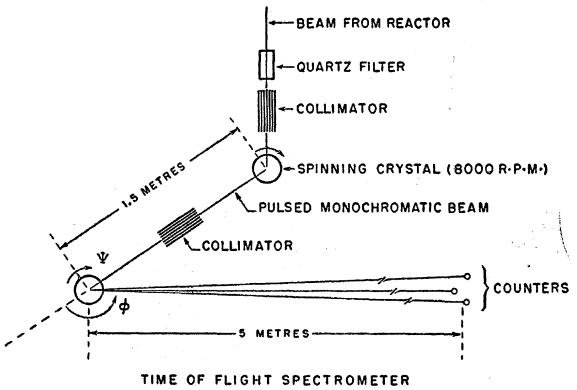

FIG. 6. Schematic layout of rotating crystal time of flight spectrometer.

[29] B. N. Brockhouse, Bull. Am. Phys. Soc. 3, 233 (1958).

phonon is increased when three counters are used. More generally, interpolation between the three counters will yield phonons in the required direction.

Typical patterns observed for the three counters for a single specimen setting are shown in Fig. 7. The main peak is elastic and arises from incoherent elastic scattering by the sodium atoms. The other peaks represent phonons. Only the strong peaks at energy gain (smaller channel number) were well enough defined to be considered useful, although the others are also shown on the accompanying reciprocal lattice diagram. The bars along the direction of $\mathbf{k}'$ represent the full width of the peaks at half maximum.

Most of the results were obtained using a multiple axis crystal spectrometer at the Chalk River *NRU* reactor. Monochromatic beams with wavelength of 1.35 A, 1.91 A and 2.22 A were used. The wavelength of 1.35 A was used chiefly for the determination of the optic modes with the neutrons losing energy in the scattering process. The beams with wavelengths of 1.91 A and 2.22 A were used at both energy loss and gain, principally for the acoustic modes. Usually the (111) plane of an aluminum crystal was used in the analyzing spectrometer but, under conditions of highest resolution, the (200) plane of the crystal was used. Some typical neutron groups are shown in Fig. 8 along with corresponding positions in the reciprocal lattice. At a wavelength of 2.22 A the full width at half maximum of the vanadium peak was 0.06 A when the (200) plane was used in the analyzing crystal.

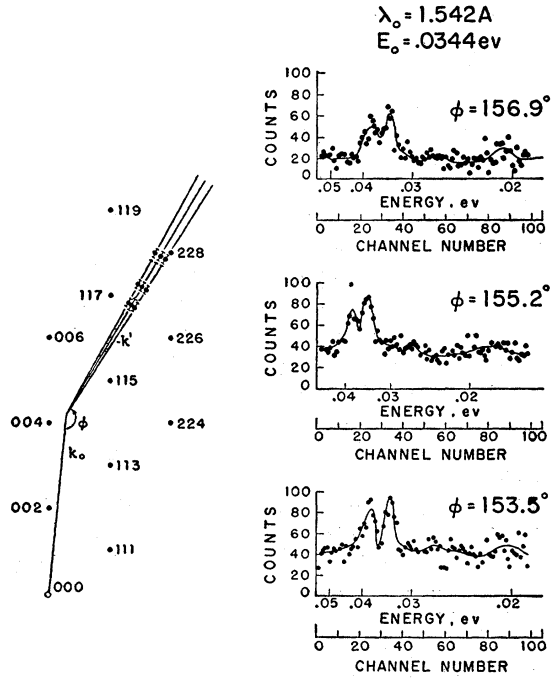

FIG. 7. Typical neutron distributions obtained with the time of flight spectrometer for a single setting of the sodium iodide crystal. The corresponding positions in the (1$\bar{1}$0) plane of the reciprocal lattice are also shown.

Two methods were used to advantage in determining the dispersion relations for the various branches. In some cases it was possible to arrange conditions so that the scattered wave vector, $\mathbf{k}'$, lay along one of the three symmetry directions and went through a reciprocal lattice point. This situation has the advantage that the direction of the observed phonon is always in the desired symmetry direction. The technique has the disadvantage that it is rarely possible to observe phonons of only one polarization and, hence, the observed neutron group often contains contributions from both longitudinal and transverse phonons if these are close in energy. For this reason the method of successive approximations was used in most of the determinations. In this method the probable energy and wave number of a desired phonon are calculated from elastic constants, theoretical models or previous results and the spectrometer set up to observe this phonon. The position in the reciprocal lattice was generally chosen so that only the phonon of the desired polarization had sufficient intensity to be observed [see the $\xi \cdot \mathbf{Q}$ term in Eq. (3.1.3)]. In general some neutron group representing a phonon is observed which may or may not have exactly the calculated energy and, hence, may not be in the desired direction. If it is not, then it is used as the basis of a calculation which is more likely to yield a phonon in this direction and, if necessary, the process can be repeated until the observed neutron group represents a phonon with the desired wave number and in the symmetry direction.

Both of these approaches were used successfully in conjunction with knowledge of the experimental elastic constants, theoretical dispersion curves (Sec. 2) and the structure factors calculated from these theoretical dispersion curves (Sec. 3). Care was taken to avoid positions in reciprocal space where mixtures of two phonons could not be resolved and where solutions of Eqs. (1.1.1) could be obtained over a range of values of $\mathbf{k}'$, the scattered wave vector.

4.2 The Acoustic Modes

Using the techniques outlined in the previous section it was, in general, quite straightforward to delineate the acoustic branches, although the high-frequency parts of the longitudinal branches, which were weak, and the complete longitudinal branch for the [110] direction offered rather more than normal difficulty. In the [110] direction it is difficult to resolve the transverse and longitudinal acoustic branches since they are not well separated in frequency. The position in the reciprocal lattice was therefore chosen so that $\xi \cdot \mathbf{Q} \approx 0$ for the transverse mode. In order to satisfy this condition the angle between $\mathbf{k}'$ and the [110] direction was always large, and phonons which were more than two or three degrees off direction often had frequencies considerably different from those which were exactly in the right direction.

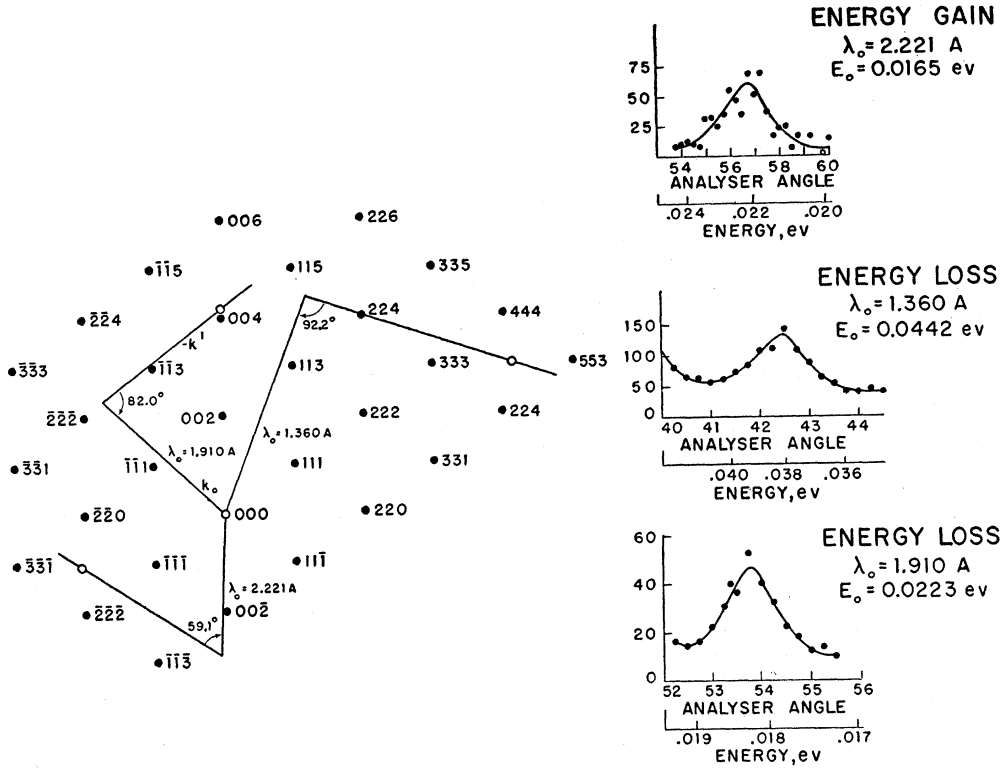

FIG. 8. Typical neutron groups observed with the crystal spectrometer together with their positions in the reciprocal lattice. The ordinate gives the number of observed counts.

In the early stages of the experiment, before the shell model for ionic crystals had been fully developed, considerable difficulty was encountered in the measurement of longitudinal acoustic phonons near the zone boundary in the [001] direction. According to the point ion model such a phonon should give an intense neutron group between even indexed points [Fig. 5(a)] but very little intensity was, in fact, observed. A strong neutron group, corresponding to this LA phonon was, however, observed between odd indexed points. When the structure factors were calculated from the shell model, it was found that just such behavior—low intensity between even points, high intensity between odd points—was predicted [Fig. 5(b)].

TABLE IV. Frequencies at selected values of q taken from smooth curves through the experimental points.

Designation	Frequency in 10^{12} cps
TA(0,0,1)	1.22±0.04
TA(0,0,$\frac{1}{2}$)	0.98±0.03
LA(0,0,1)	1.82±0.06
LA(0,0,$\frac{1}{2}$)	2.00±0.06
TA($\frac{1}{2},\frac{1}{2},\frac{1}{2}$)	1.52±0.05
TA($\frac{1}{4},\frac{1}{4},\frac{1}{4}$)	1.08±0.04
LA($\frac{1}{2},\frac{1}{2},\frac{1}{2}$)	2.32±0.06
LA($\frac{1}{4},\frac{1}{4},\frac{1}{4}$)	1.73±0.05
TA($\frac{1}{2},\frac{1}{2}$,0)	1.40±0.05
LA($\frac{1}{2},\frac{1}{2}$,0)	2.16±0.06
TO(0,0,0)	3.6_0 ±0.1
TO(0,0,1)	3.8_0 ±0.1
TO($\frac{1}{2},\frac{1}{2},\frac{1}{2}$)	3.5_0 ±0.1
LO(0,0,0)	5.0 ±0.5
LO(0,0,1)	3.9_1 ±0.1

The measurements of the dispersion relations for all modes are shown in Fig. 2. Values of the frequencies at selected points are shown in Table IV. The optic modes will be discussed later. Figure 2 also includes curves which have been calculated from two theoretical models —the point ion model and the shell model of Sec. 2. The straight lines in Fig. 2 represent the appropriate velocities of sound calculated from the elastic constants measured by Dalven and Garland.[25] Their results have been extrapolated to 110°K (from 180°K) using as a guide the temperature dependence of the elastic constants of other alkali halides.[30] It can be seen that for long wavelengths ($q \rightarrow 0$) the slope of the neutron curves agree well with the velocities calculated from these elastic constants.

An interesting feature of these curves is the dip in the longitudinal branch in the [001] direction as the zone boundary is approached. This effect is predicted by the shell model but not by the point ion model.

The individual errors for the points are not shown on these curves. The absolute error in any one determination is difficult to estimate properly.[3,5] It is felt that the scatter in the points is a good indication of the size of the

[30] M. H. Norwood and C. V. Briscoe, Phys. Rev. **112**, 45 (1958).

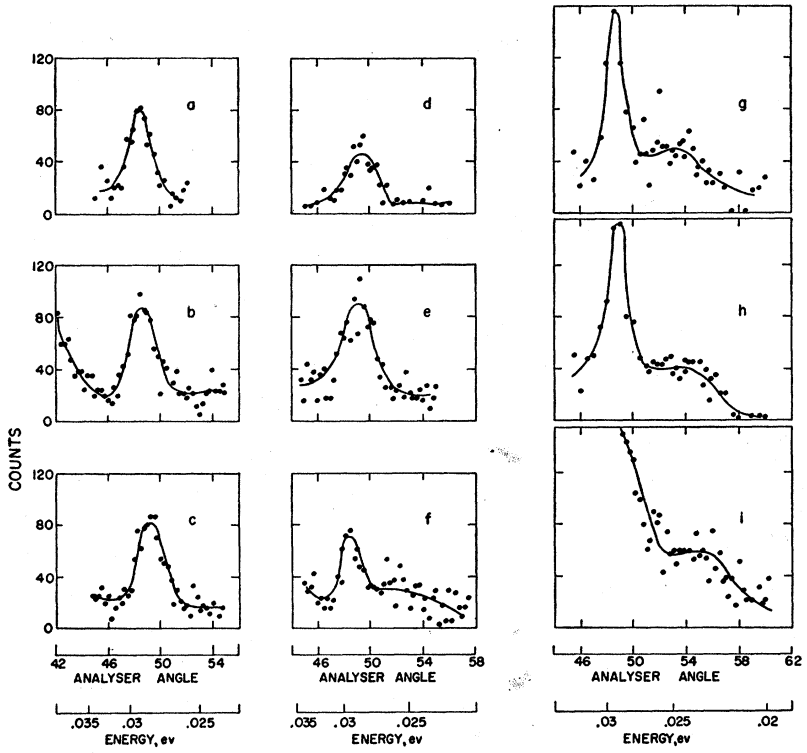

FIG. 9. Neutron groups representing optical vibrations observed in the [001] and [110] directions. These groups contain a contribution from inelastic incoherent scattering by the sodium ions. The initial energy of the neutrons was 0.0442 ev.

errors. Each of the acoustic branches is probably defined to an accuracy of about 3% (the error in the energy determinations of single phonons is often less than this).

4.3 The Optic Modes

The measurements of the frequencies of the optic modes is complicated by the effects of the large incoherent scattering cross section of sodium. Not only is there a large elastic peak arising from this incoherent scattering but also the thermal vibrations give rise to inelastic incoherent scattering. If there are not many modes with the same frequency then the incoherent contribution to the neutron group representing a phonon is not great. However, if a branch of the dispersion relations is nearly flat for all directions of $\mathbf{q}$ then many modes will contribute to the incoherent inelastic scattering for this frequency. As a result there will be a peak in the scattered neutron distribution which is independent of polarization and wave number and depends only on the momentum transfer, $|\mathbf{Q}|$, and other factors, such as temperature, which are constant in a given series of experiments. This can also be expressed by saying that the scattered incoherent inelastic intensity depends on $g(\nu)$, the fraction of normal modes between ν and $\nu+d\nu$, a well-known result.[11] [This intensity, however, does not depend only on $g(\nu)$; see discussion in Sec. 3.2.]

Such a peak is indeed observed at positions in reciprocal space where, by reason of the polarization and structure factors, coherent scattering with an energy change corresponding to the transverse optic modes would be forbidden. This incoherent neutron group contaminates the peaks representing desired phonons in the optic branches and must be subtracted from them before the details of these branches can be determined.

Figure 9 shows a series of neutron groups corresponding to phonons in the [110] and [001] directions. The positions of these neutron groups in $\mathbf{Q}$ space (after the incoherent contribution was subtracted) is shown on the reciprocal lattice diagram in Fig. 10. It can be seen that in the [110] direction only transverse phonons could be excited (the angle between $\mathbf{Q}=\mathbf{k}_0-\mathbf{k}'$ and $\mathbf{q}$ being nearly 90°) and that in the [001] direction longitudinally polarized phonons were favored. As $\mathbf{q}$ becomes smaller in the [001] direction the structure factor for the longitudinal phonons decreases rapidly between even indexed points in reciprocal space and increases correspondingly between odd indexed points (Fig. 5). For this reason the line which was being followed in reciprocal space was changed between group *e* and group *f*. All of these peaks contain a contribution from the incoherent inelastic scattering described above which must be subtracted quantitatively if the results are to be meaningful.

The behavior of this inelastic incoherent scattering was accordingly determined. As far as one could tell the shape of the peak was the same for all values of $|\mathbf{Q}|$ and thus the peak height was the only parameter necessary to determine this incoherent intensity once the energy (or the spectrometer angle) distribution had been deter-

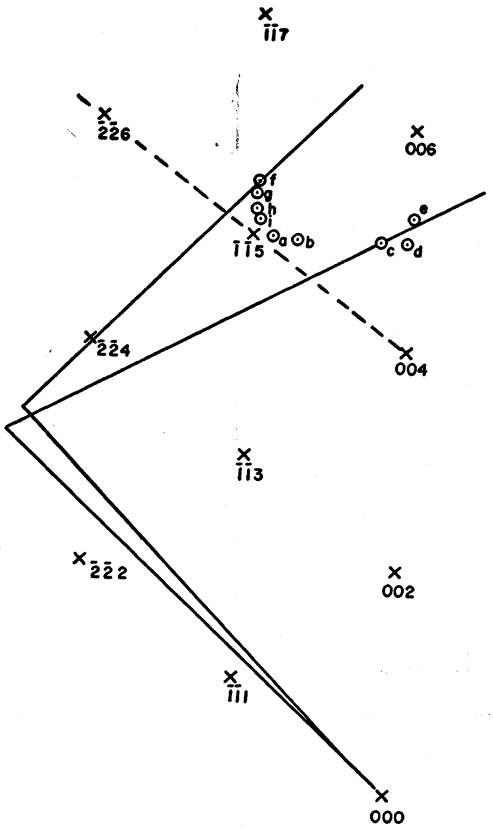

FIG. 10. The $(1\bar{1}0)$ plane of the reciprocal lattice showing the position in reciprocal space of the phonons represented by the neutron groups in Fig. 9. Group a was actually observed at the same $\mathbf{q}$ but not the same $\mathbf{Q}$ as shown here.

mined from a single curve. The points on this curve had only to be multiplied by the appropriate peak intensity before subtracting it, point by point, from the neutron groups in Fig. 9. The result of this subtraction procedure is shown in Fig. 11.

In Sec. (3.2) it was shown that the ratio of the incoherent intensity to the coherent intensity should be about 0.8 for the case of most favorable polarization. This ratio has been computed for twelve observed transverse optic phonons with the result that

$$I_{\text{incoh}}/I_{\text{coh}}=0.85\pm0.1.$$

The assumptions made in deducing the theoretical value for this ratio were such as to make 0.8 an upper limit so that the observed value of 0.85 ± 0.1 is probably significantly higher than the exact theoretical value. Such a behavior is, however, to be expected since part of the contribution to the inelastic incoherent peak is from multiple scattering: inelastic incoherent or coherent scattering from a transverse optic mode plus elastic incoherent scattering.

Figures 2 and 11 show the behavior of the optic branches. Along the transverse optic branch in the [110] direction the frequency increases slightly with increasing $\mathbf{q}$. However, neither the width nor the intensity of the neutron distribution changes significantly as $\mathbf{q}$ is increased to the point where the [110] transverse branch joins the [001] longitudinal branch at the [001] zone boundary. As $\mathbf{q}$ decreases for the longitudinal optic branch in the [001] direction the peak height begins to decrease and the width to increase until what were once well-defined neutron groups indicating phonons become broad distributions which are difficult to interpret (Sec. 5). Further observations are obscured by a transverse optic phonon whose intensity is increasing because of increasingly favorable polarization and structure factors. This contributes appreciably to the broadened distribution which supposedly represents the desired longitudinal optic phonon. On the assumption that the center of this distribution represents such a phonon, the energy and wave number have been calculated and are shown in Fig. 2 along with the other branches.

Because of the difficulties in obtaining these results, the other longitudinal optic branches were not studied in detail at this time although some indications of phonons in these branches near the zone boundaries in the [110] and [111] directions have been observed. Two points in the [110] direction were obtained by the methods outlined above and are included in Fig. 2. In the observations of the longitudinal phonons in the [001] direction and of the transverse phonons in the [110] direction there is considerable intensity at large energy transfers (groups c and f, Fig. 11). The corresponding positions in reciprocal space have a large $\mathbf{q}$ in the [111] direction. The wings of the curves (for example group h) are much less intense when the corresponding energy transfers take place at other positions in reciprocal space. This result probably indicates that the frequency of the longitudinal optic branch in the [111] direction increases with increasing $\mathbf{q}$, as predicted by the shell model.

The transverse optic branches were, in general, well defined and were almost flat in all directions. At $q=0$ the measured transverse optic frequency of 3.6×10^{12} cps (at 110°K) agrees satisfactorily with the infrared absorption frequency of 3.5×10^{12} cps measured at room temperature.[31] The errors in the determination of the energy of the phonons in these branches are also believed to be about 3%.

5. DISCUSSION

There is generally good agreement between the measured dispersion relations of Fig. 2 and the dispersion relations calculated on the simple version of the shell model—Coulomb forces between ions of unit charge with the iodine atoms polarizable, and central repulsive forces between first neighbors only, acting through the iodine shell. The root-mean-square deviation between theory and experiment is about 7%. In

[31] R. B. Barnes, Z. Physik **75**, 723 (1932).

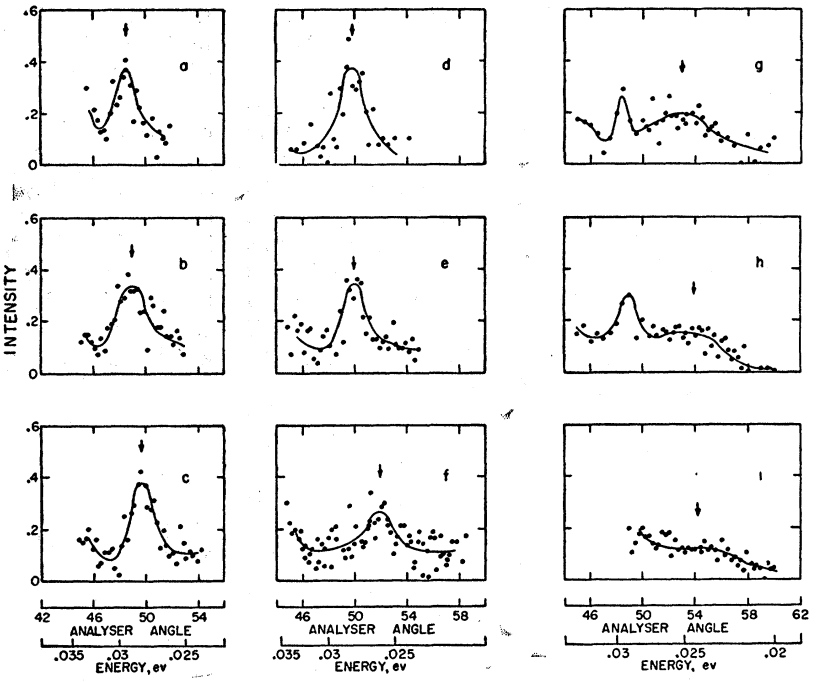

FIG. 11. The neutron groups of Fig. 9 with the inelastic incoherent contribution subtracted as explained in the text.

assessing this agreement it should be recalled that *no free parameters* were used to fit the neutron data, the parameters of the model being fixed by the elastic constant c_{11} and by the high- and low-frequency dielectric constants. We consider that the agreement verifies that the general picture is correct.

There are, however, real discrepancies existing between theory and experiment, especially in the LA mode near the zone boundary in the [111] direction (the point $\frac{1}{2}, \frac{1}{2}, \frac{1}{2}$). It would be of interest to try to assign physical origins to these discrepancies and thus to see in what ways the simple model could be improved.

One significant fact is that on the acoustic branches the experimental points in every case lie between the curves for the point ion model and the shell model, although they are closer to the latter. Thus these branches seem to be overcorrected for the effects of polarizability. On the simple model this could only be improved at the price of no longer fitting the dielectric constants and violating the theorem (strongly based on macroscopic theory) that the ratio of the longitudinal and transverse optic frequencies at $q=0$ is equal to $(\epsilon_0/\epsilon)^{\frac{1}{2}}$. Some modifications to the model itself are therefore indicated.

A possible modification is suggested by the discrepancy in the mode LA$(\frac{1}{2},\frac{1}{2},\frac{1}{2})$. The iodine ions in NaI are much larger (ionic radius 2.20 A) than the sodium ions (1.00 A)[32] and it is quite likely that there is a small direct interaction between nearest neighbor iodine ions. In the mode LA$(\frac{1}{2},\frac{1}{2},\frac{1}{2})$ only the iodine ions move, near (like) neighbors against each other. The sodium ions remain fixed as a consequence of symmetry. It is therefore reasonable that this frequency should be raised by a small iodine-iodine interaction.

If, however, we simply introduce second neighbor force constants between iodine ions (Appendix A2) to reconcile theory and experiment for LA$(\frac{1}{2},\frac{1}{2},\frac{1}{2})$ then the agreement is made worse at other points and other small changes are necessary. One such change is the introduction of noncentral forces between first neighbors. Such noncentral forces are thought to be small, however, since the Cauchy relation $c_{12}=c_{44}$ is approximately satisfied for NaI at 110°K. This argument cannot be considered sufficient, however, since the uncertainty in the experimental value of c_{12} is of the order of 15%[24] and also deviations from the Cauchy relation up to 20% are observed at other temperatures. It is therefore probable that both iodine-iodine interactions and noncentral forces between first neighbors should be included in any more realistic model of sodium iodide. We have not yet made a complete investigation of the effects of introducing these secondary interactions or of varying the ionic charge Ze but further work is being done on the alkali halides and we hope to make such an investigation in the near future. For the present it appears, from inspection of the equations (Appendix A2) and the results, that these subsidiary interactions are probably less than 10% of the central first neighbor interaction and that the ionic charge, Ze, is probably greater than $0.95e$. (It should be noted that the definition of ionic charge involved here is such that when $Z=1$ there is no covalent bonding. It is not the same

[32] See R. W. G. Wyckoff, *Crystal Structures* (Interscience Publishers, Inc., New York, 1948), Vol. I, Chap. III, p. 15.

as the "effective charge" discussed in Sec. 2 and elsewhere, which refers to the effect of distortion polarizability on the optic frequencies at $q=0$.)

As was stated in Sec. 4, considerable difficulty was encountered in measuring the LO vibrations. We made several attempts, at 110°K and also at room temperature, under conditions for which we thought sharp neutron groups should be obtained. In every case a quasi-continuous distribution of scattered neutrons was observed. In the particular case of the experiments shown in Figs. 10 and 11 there is a geometrical reason for some broadening of the neutron groups. In Fig. 10 if $\mathbf{k}'$ is shortened, $\mathbf{q}$ is shortened and ν increased; if $\mathbf{k}'$ is lengthened, $\mathbf{q}$ is lengthened and ν decreased. But in the LO dispersion curve ν decreases as $\mathbf{q}$ increases, and vice versa. Thus there is a range of values of $\mathbf{k}'$ which satisfy Eqs. (1.1.1) and a broad neutron group is expected. Nevertheless, we are convinced that the broadening is too great to be accounted for by this mechanism. Furthermore we have made several measurements under the opposite conditions, without observing any neutron groups except very broad ones. We therefore believe the broadening of the LO modes to be real, and probably to arise from interaction between the modes. The energy broadening would then be related via the uncertainty principle to the lifetime of the vibrations.[33] If this is the correct explanation of our observations then in NaI at the low temperature of 110°K the longer wavelength longitudinal optic modes have very short lifetimes. The results are not sufficiently accurate to allow good values for the lifetimes to be given, but they appear to be of the order of the vibrational period.

It will be noted from Fig. 2 that the frequencies obtained from Eqs. (1.1.1) by using the wave vector and energy corresponding to the center of the broad group are lower than the frequencies calculated on the shell model. The value extrapolated to $q=0$ is also less than is given by $\omega_L=\omega_T(\epsilon_0/\epsilon)^{\frac{1}{2}}$. This is explicable on the lifetime hypothesis; a dissipative term in the differential equation for a harmonic oscillator lowers the frequency.

We have no detailed explanation for this short lifetime but offer the following argument. The longitudinal optical modes have associated with them a much higher macroscopic electric field than do the other branches. Furthermore, the energy of the mode with $q=0(\lambda\rightarrow\infty)$ is sensitive to the shape of the crystal if $\lambda\rightarrow\infty$ faster than do the dimensions of the crystal. In fact, for a spherical crystal of finite size there is only one triply degenerate mode with $q=0$ and the distinction between longitudinal and transverse modes is no longer possible.[34] These are electrostatic surface effects. In a similar way the energies of the LO modes may be especially sensitive to the termination of the wavetrain by interaction with other phonons.

We are now attempting to study the behavior of the optical branches in more detail using a specimen of potassium bromide. With potassium bromide the intensities are higher than with sodium iodide, and the contaminant incoherent scattering is much smaller. We hope to be able to verify the energy broadening of the LO modes, and to study it in detail under more favorable conditions than existed for the experiments described above. This work will be made easier by a new apparatus which enables energy distributions to be taken at constant $\mathbf{Q}$ and thus to avoid the geometrical effects discussed above.

ACKNOWLEDGMENTS

The authors are grateful to E. A. Glaser for technical assistance, and to Dr. J. M. Kennedy and Miss M. Millican for machine computations.

APPENDIX 1. THE ELASTIC CONSTANTS

We now consider the effect of polarizability on acoustic modes having a small value of $\mathbf{q}$, that is, the effect on the elastic constants. By expanding $A(11)$, $A(22)$, and $A(12)$ of Eqs. (2.2.11) as a power series in q^2, it is found that this equation reduces to

$$\omega^2=\frac{A_2(11)+A_2(22)+2A_2(12)}{m_1+m_2}, \quad \text{for} \quad q\rightarrow 0,$$

where for example, $A_2(11)$ is the coefficient of the term in q^2 in the expression of $A(11)$. In deriving this expression use is made of invariance relations for the A's similar to Eqs. (2.2.5).

When $\mathbf{q}$ is in a symmetry direction

$$\omega^2=q^2(c/\rho),$$

where ρ is the density of the material and c is a linear combination of the elastic constants c_{11}, c_{12}, and c_{44}. Hence, we find that

$$c=-\frac{1}{v}\lim_{q\rightarrow 0}\left[\frac{A(11)+A(22)+2A(12)}{q^2}\right]. \quad \text{(A.1.1)}$$

On substituting the appropriate values of $A_2(11)$, etc., we find

$$c=-\frac{2}{v}\lim_{q\rightarrow 0}\left[\frac{R_0+R+(Z^2e^2/v)(C_1-C_2)+\text{terms in } q^4, \text{ etc.}}{q^2}\right].$$

On taking the limit $q\rightarrow 0$ we obtain the same result as is obtained when polarizability is excluded. It is not difficult to show that the result is still true when both ions are polarizable. The elastic constants are therefore unaffected by the use of a shell model. This agrees with the conclusions of Szigeti[35] and of Herpin[36] that polari-

[33] The possibility of observing a broadening of the neutron groups because of a lifetime for the phonons was pointed out several years ago by G. Placzek (private communication via G. L. Squires). It has recently been discussed in a formal way by L. Van Hove, Massachusetts Institute of Technology Technical Report No. 11, 1959 (unpublished).

[34] H. Frohlich, *Theory of Dielectrics* (Oxford University Press New York, 1949), Sec. 8.

[35] B. Szigeti, Proc. Roy. Soc. (London) **A204**, 51 (1950).

[36] A. Herpin, J. phys. radium **14**, 611 (1953).

zability does not affect the elastic constants when each each ion occupies a center of symmetry.

APPENDIX 2. EFFECT OF SECOND NEIGHBOR AND NONCENTRAL FIRST NEIGHBOR INTERACTIONS

We consider briefly in this section the effect of introducing a short-range interaction between the negative ions (second neighbors). It is readily shown that, provided this interaction is relatively weak, it does not matter whether it acts through the shells or through the cores, so that we treat it as a force between rigid ions. We take this force also to be a central force. We simplify the notation of Eq. (2.1.1) by writing $V_{12}(r_0)$ for $\Phi^{(R)}(r_0)$, and add a potential $V_{22}(r_1)$ between negative ions. We then have

$$U_0=-\alpha_M(Z^2e^2/r_0)+6V_{12}(r_0)+6V_{22}(r_1). \quad \text{(A.2.1)}$$

(The coefficient of V_{22} is not twelve but six; although each negative ion is surrounded by twelve like ions there are twice as many 1−2 interactions as there are 2−2 interactions.)

Using symbols such as $(\partial V_{12}/\partial r)_{\parallel}$ for the potential gradients shown in Fig. 1(b), the previous definitions, (2.1.2), take the form

$$\left(\frac{\partial^2 V_{12}}{\partial r^2}\right)_{\parallel}\Bigg|_{r=r_0}=\frac{e^2A}{2v},$$

and

$$\frac{1}{r_0}\left(\frac{\partial V_{12}}{\partial r}\right)_{\parallel}\Bigg|_{r=r_0}=\left(\frac{\partial^2 V_{12}}{\partial r^2}\right)_{\perp}\Bigg|_{r=r_0}=\frac{e^2B}{2v}. \quad \text{(A.2.2)}$$

Similarly we define

$$\left(\frac{\partial^2 V_{22}}{\partial r^2}\right)_{\parallel}\Bigg|_{r=r_1}=\frac{e^2A'}{2v},$$

and

$$\frac{1}{r_1}\left(\frac{\partial V_{22}}{\partial r}\right)_{\parallel}\Bigg|_{r=r_1}=\left(\frac{\partial^2 V_{22}}{\partial r^2}\right)_{\perp}\Bigg|_{r=r_1}=\frac{e^2B'}{2v}. \quad \text{(A.2.3)}$$

The stability condition $(\partial U_0/\partial r)_{r=r_0}=0$ now gives the result

$$B+2B'=-\tfrac{2}{3}\alpha_M Z^2. \quad \text{(A.2.4)}$$

On considering the effect of these additional force constants on the coefficients $R_{xy}(\kappa\kappa')$ it is found that further terms are added when $\kappa\kappa'=22$, but all others are unchanged. Using methods similar to those described by de Launay[37] it is found that the additional terms are, for example

$$\begin{aligned}\Delta R_{xx}(22)=(e^2/v)[&2A'+4B'\\&-A'\cos q_x r_0(\cos q_y r_0+\cos q_z r_0)\\&-B'(2\cos q_y r_0\cos q_z r_0\\&+\cos q_x r_0\cos q_y r_0+\cos q_x r_0\cos q_z r_0)],\end{aligned}$$

and

$$\Delta R_{xy}(22)=(e^2/v)(A'-B')\sin q_x r_0\sin q_y r_0. \quad \text{(A.2.5)}$$

[37] J. de Launay, *Solid State Physics*, edited by F. Seitz and J. Turnbull (Academic Press, Inc., New York, 1956), Vol. 2.

Using the expressions given in Table I we can find the amount by which $A(22)$ of Eq. (2.2.11) is changed when $\mathbf{q}$ is in any symmetry direction. We may also find the effect on the elastic constants by using Eq. (A.1.1). For example, when $\mathbf{q}=(q_x,0,0)$, Eq. (A.1.1) gives $c=c_{11}$ for a longitudinal mode, $c=c_{44}$ for a transverse mode. In this way we find, when Eq. (A.2.4) is taken into account, that

$$\begin{aligned}c_{11}&=(e^2/2r_0^4)[-2.555z^2+\tfrac{1}{2}(A+A'+B')],\\c_{12}&=c_{44}=(e^2/2r_0^4)[0.696Z^2+\tfrac{1}{4}(A'-B')].\end{aligned} \quad \text{(A.2.6)}$$

These give

$$\beta^{-1}=\tfrac{1}{3}(c_{11}+2c_{12})=(e^2/6r_0^4)(-1.163Z^2+\tfrac{1}{2}A+A').$$

This result may be checked by evaluating the compressibility directly, using the result

$$\beta^{-1}=\frac{1}{18r_0}\left(\frac{\partial^2 U_0}{\partial r^2}\right)_{r=r_0}.$$

When $A'=B'=0$ and $Z=1$ the above results reduce to those given by Kellermann.

If we add a noncentral component to the force between nearest neighbors, the condition

$$\frac{1}{r_0}\left(\frac{\partial V_{12}}{\partial r}\right)_{\parallel}\Bigg|_{r=r_0}=\left(\frac{\partial^2 V_{12}}{\partial r^2}\right)_{\perp}\Bigg|_{r=r_0}$$

no longer holds, so we write

$$\left(\frac{\partial^2 V_{12}}{\partial r^2}\right)_{\perp}\Bigg|_{r=r_0}=\frac{e^2(B+B'')}{2v},$$

while

$$\frac{1}{r_0}\left(\frac{\partial V_{12}}{\partial r}\right)_{\parallel}\Bigg|_{r=r_0}=\frac{e^2B}{2v}$$

as before. It is then found that c_{11} is unchanged, while

$$\begin{aligned}c_{12}&=(e^2/2r_0^4)(0.696Z^2-\tfrac{1}{4}B'+\tfrac{1}{4}A'-\tfrac{1}{2}B''),\\c_{44}&=(e^2/2r_0^4)(0.696Z^2-\tfrac{1}{4}B'+\tfrac{1}{4}A'+\tfrac{1}{2}B'').\end{aligned} \quad \text{(A.2.7)}$$

The effect on the coefficients $R_{xx}(12)$, etc., is to replace B everywhere by $B+B''$.

APPENDIX 3. LATTICE DYNAMICS AND DIELECTRIC PROPERTIES WITH BOTH IONS POLARIZABLE

The results which were given in Sec. 2 should be adequate for sodium iodide, where the polarizability of the sodium ion is relatively very small. It is, however, of some interest to consider the solution of Eqs. (2.2.7) when both ions are polarizable, particularly for $q=0$ where the results are closely connected with the dielectric properties of the crystal. The exact result for the optic modes is found to be

$$(\mu\omega^2)_{q=0}=R_0'+\frac{C_1(Z'e)^2}{v+\alpha C_1},$$

where

$$R_0'=R_0-\frac{T_0^2(k_1+k_2+2F_0)}{(k_1+F_0)(k_2+F_0)+S_0(k_1+k_2+2F_0)},$$

$$Z'=Z+\frac{T_0[Y_2(k_1+F_0)-Y_1(k_2+F_0)]}{(k_1+F_0)(k_2+F_0)+S_0(k_1+k_2+2F_0)}, \quad \text{(A.3.1)}$$

and

$$\alpha=\frac{e^2[(k_2+F_0)Y_1^2+(k_1+F_0)Y_2^2+S_0(Y_1+Y_2)^2]}{(k_1+F_0)(k_2+F_0)+S_0(k_1+k_2+2F_0)}.$$

It may be shown that it is the quantity α which determines the high-frequency dielectric constant, ϵ, of the crystal, through the equation

$$\frac{\epsilon-1}{\epsilon+2}=\frac{4\pi\alpha}{3v}. \quad \text{(A.3.2)}$$

When α is calculated in terms of the dipole moments of the individual atoms, it is found that

$$\alpha_1=e^2\left[\frac{Y_1^2}{k_1+T_0}+\frac{S_0Y_1Y_2}{(k_1+T_0)(k_2+T_0)}\right]\div\left[1-\frac{S_0^2}{(k_1+T_0)(k_2+T_0)}\right],$$

$$\alpha_2=e^2\left[\frac{Y_2^2}{k_2+T_0}+\frac{S_0Y_1Y_2}{(k_1+T_0)(k_2+T_0)}\right]\div\left[1-\frac{S_0^2}{(k_1+T_0)(k_2+T_0)}\right], \quad \text{(A.3.3)}$$

whereas before $T_0=S_0+F_0$, and comparison with Eq. (A.3.1) then shows that $\alpha=\alpha_1+\alpha_2$, as expected. However, only when $S_0=0$ do we have α_1 independent of the parameters of atom 2, and vice versa, when in fact

$$\alpha_1=\frac{Y_1^2e^2}{k_1+F_0}, \qquad \alpha_2=\frac{Y_2^2e^2}{k_2+F_0}.$$

[These are the values of α_κ which appear in Eq. (2.2.9)]. For our present purpose it is in fact more convenient to define a slightly different polarizability α_1 which is also independent of the parameters of atom 2, and is given by

$$\alpha_1=\frac{Y_1^2e^2}{k_1+T_0}, \text{ and similarly } \alpha_2=\frac{Y_2^2e^2}{k_2+T_0}.$$

When k_1 and k_2 are large compared with S_0 (as appears likely to be generally true, since in sodium iodide $k_1\gg k_2\approx 10S_0$) these values of α_1 and α_2 give $\alpha=\alpha_1+\alpha_2$ to within a few percent, and may be referred to as the atomic polarizabilities, without qualification. By analogy with Eq. (2.3.3) we define

$$d_1=\frac{-T_0Y_1}{k_1+S_0+F_0}, \quad d_2=\frac{-T_0Y_2}{k_2+F_0+S_0}. \quad \text{(A.3.4)}$$

Both are positive quantities, and are measures of the distortion polarizabilities of the positive and the negative ion, respectively. Equation (A.3.1) may then be written [see Eqs. (2.3.5) to (2.3.7)]

$$\mu\omega_T^2=R_0'-4\pi(\epsilon+2)(Z'e)^2/9v,$$
$$\mu\omega_L^2=R_0'+8\pi(\epsilon+2)(Z'e)^2/9v\epsilon,$$

where the primed quantities can be expressed approximately in terms of quantities associated with individual ions as follows:

$$R_0'=R_0-e^2\left(\frac{d_1^2}{\alpha_1}+\frac{d_2^2}{\alpha_2}\right), \quad \text{(A.3.5)}$$
$$Z'=Z+d_1-d_2.$$

Use of the result $\omega_L^2/\omega_T^2=\epsilon_0/\epsilon$ then leads to the following exact relations,

$$\epsilon_0-\epsilon=4\pi(\epsilon+2)^2(Z'e)^2/9v\mu\omega_T^2, \quad \text{(A.3.6)}$$

and

$$R_0'=\mu\omega_T^2[(\epsilon_0+2)/(\epsilon+2)]. \quad \text{(A.3.7)}$$

If only first neighbor atoms interact, the result $R_0=6r_0/\beta$ should also hold. These results are to be compared with those given by Szigeti[35,38]; (A.3.6) is in principle the same while (A.3.7) differs through the replacement of R_0 by R_0'. The difference between these two quantities, $e^2(d_1^2/\alpha_1+d_2^2/\alpha_2)$, is comparatively small ($\sim$10%) for alkali halides. Results similar to those given here have been obtained by Hanlon and Lawson.[19] If the forces between ions act entirely through the shells, $F=D=0$ and $T=S=R$. The quantity d_1, for example, is then given by

$$d_1=-R_0Y_1/(k_1+R_0)\approx -R_0Y_1/k_1.$$

One might therefore expect d_1/R_0 to be characteristic of a particular ion, and not of the alkali halide in which it occurs. The extent to which Eqs. (A.3.6) and (A.3.7) agree with observation when this assumption is made, and with $Z=1$, has been briefly considered elsewhere[39]; quite good agreement was found.

If we assume further that the shells carry the same charge, as appears to be the case from the work of Hanlon and Lawson, we may write as an abbreviation $\gamma=-(Y_1e)^{-1}=-(Y_2e)^{-1}$. Equation (A.3.1) then gives exactly

$$\mu\omega_T^2=R_0-\frac{T_0^2\gamma^2(\alpha_1+\alpha_2-2S_0\gamma^2\alpha_1\alpha_2)}{1-S_0^2\gamma^4\alpha_1\alpha_2}-\frac{4\pi(\epsilon+2)}{9v}\left[Ze-\frac{T_0\gamma(\alpha_2-\alpha_1)}{1-S_0^2\gamma^4\alpha_1\alpha_2}\right]^2, \quad \text{(A.3.8)}$$

[38] B. Sziegeti, Trans. Faraday Soc. 45, 155 (1949).
[39] W. Cochran, Phil. Mag. 4, 1082 (1959).

with a similar expression for $\mu\omega_L^2$. Thus the coefficient R_0 is effectively reduced by an amount approximately proportional to the sum of the polarizabilities, and the ionic charge Ze by an amount proportional to their difference. The latter conclusion agrees with that of Hanlon and Lawson, who show that the result holds rather well in practice. A short calculation, which we omit, shows that when in the course of an optic vibration having $q=0$ the nuclei are displaced a relative distance $\mathbf{u}$, the polarization of the medium is $\mathbf{P}=Z'e/(v+\alpha C_1)\mathbf{u}$, that is

$$\mathbf{P}=\frac{(\epsilon+2)Z'e}{3v}\mathbf{u}(\mathrm{TO}) \quad \text{and} \quad \mathbf{P}=\frac{(\epsilon+2)Z'e}{3v\epsilon}\mathbf{u}(\mathrm{LO}). \quad \text{(A.3.9)}$$

The effective field in the crystal is found to be given by $\mathbf{E}=-C_1\mathbf{P}$, that is $+(4\pi/3)\mathbf{P}(\mathrm{TO})$ and $-(8\pi/3)\mathbf{P}(\mathrm{LO})$. This latter value may be regarded as the sum of components $+(4\pi/3)\mathbf{P}$ and $-4\pi\mathbf{P}$, the term $-4\pi\mathbf{P}$ being the contribution of the macroscopic field in the crystal.[16] In all respects the ions act in optic vibrations for which $q=0$ (or in an externally-applied field) as if their charges were $\pm Z'e$, instead of $\pm Ze$. This is not so for general values of $\mathbf{q}$ however.

Using numerical results given elsewhere[39] one can show that the term $e^2(d_1^2/\alpha_1+d_2^2/\alpha_2)$ is about 10% of R_0 at most for alkali halides, while $(Z')^2(\epsilon+2)/3$ varies from 0.7 for KI to 1.05 for NaF, with an average value of about 0.85. It is then found that to quite a fair approximation, for all alkali halides,

$$\begin{aligned}\mu\omega_T^2&=R_0'-4\pi(\epsilon+2)(Z'e)^2/9v\\&\approx R_0-4\pi e^2/3v=(e^2/v)(A+2B-4\pi/3). \quad \text{(A.3.10)}\end{aligned}$$

This latter value is, however, the result obtained by Kellermann,[15] neglecting polarizability. The fact that Eq. (A.3.10) gives a value for ω_T in fair agreement with observation has been a source of confusion, and has, for example, led to the erroneous conclusion that the Lorentz formula for the effective field $(E_0+4\pi P/3)$ is invalid in alkali halide crystals.[40] The explanation which we give here of the apparent validity of (A.3.10) has been advanced previously,[16,35] but in somewhat different terms. Although it is not immediately obvious from Eqs. (2.3.4), in sodium iodide the mutual cancellation of the effects of "field polarizability" and "distortion polarizability" applies to a large extent in all modes of vibration except the longitudinal optic.

Finally, we give the general solution of Eqs. (2.2.7) in a form which is probably adequate for the alkali halides, by setting $F=0$, $Z=1$ and assuming that S_0 is small compared with k_1 or k_2. For an alkali halide we need not distinguish between C_2 and C_2^*, etc., since each ion is on a center of symmetry. The result is that in the characteristic Eq. (2.2.11),

$$\begin{aligned}A(11)&=R_0-\frac{e^2}{f}\left(\frac{d_1^2}{\alpha_1}+\frac{S^2}{S_0^2}\frac{d_2^2}{\alpha_2}\right)\\&\quad+\frac{e^2}{fv}\Bigg[C_1\left(1-d_1^2\frac{\alpha_2}{\alpha_1}-\frac{S^2}{S_0^2}d_2^2\frac{\alpha_1}{\alpha_2}+2d_1\right)\\&\quad+2C_2d_2\frac{S}{S_0}(1+d_1)+\frac{\alpha_2}{v}(1+2d_1)(C_1^2-C_2^2)\Bigg]\\A(22)&=R_0-\frac{e^2}{f}\left(\frac{d_2^2}{\alpha_2}+\frac{S^2}{S_0^2}\frac{d_1^2}{\alpha_1}\right)\\&\quad+\frac{e^2}{fv}\Bigg[C_1\left(1-d_2^2\frac{\alpha_1}{\alpha_2}-\frac{S^2}{S_0^2}d_1^2\frac{\alpha_2}{\alpha_1}-2d_2\right)\\&\quad-2C_2d_1\frac{S}{S_0}(1-d_2)+\frac{\alpha_1}{v}(1-2d_2)(C_1^2-C_2^2)\Bigg],\\A(12)&=A(21)=R-\frac{e^2}{f}\frac{S}{S_0}\left(\frac{d_1^2}{\alpha_1}+\frac{d_2^2}{\alpha_2}\right)\\&\quad+\frac{e^2}{fv}\Bigg\{-C_2\left[1-\left(1+\frac{S^2}{S_0^2}\right)d_1d_2\right]\\&\quad-C_1\frac{S}{S_0}\left(d_1^2\frac{\alpha_2}{\alpha_1}+d_2^2\frac{\alpha_1}{\alpha_2}\right)+\left(C_1\frac{S}{S_0}-C_2\right)(d_1-d_2)\Bigg\},\end{aligned}$$

where as before (with $F_0=0$)

$$\alpha_1=\frac{Y_1^2e^2}{k_1+S_0}, \quad \alpha_2=\frac{Y_2^2e^2}{k_2+S_0}, \quad d_1=-\frac{S_0Y_1}{k_1+S_0}, \quad d_2=-\frac{S_0Y_2}{k_2+S_0},$$

and f is now an abbreviation for

$$\left[1+\frac{C_1}{v}(\alpha_1+\alpha_2)+\frac{\alpha_1\alpha_2}{v^2}(C_1^2-C_2^2)\right].$$

On the reasonable assumptions that the forces act through the shells, and that these carry equal charges, all the parameters in the above expressions can be determined from ϵ_0, ϵ, and β (or c_{11}). We have not yet been able to test the validity of these expressions experimentally, since in sodium iodide the polarizability of the positive ion is very small ($\alpha_1\approx 0.03\alpha_2$) and Eq. (2.3.4) is thus an adequate approximation.

[40] N. F. Mott and R. W. Gurney, *Electronic Processes in Ionic Crystals* (Oxford University Press, New York, 1948).